CONTRACT SERIAL NUMBER 79054-01-SQ
CONTRACTOR: MCGILL UNIVERSITY
CONTRACT REQUISITION NUMBER 23440-7-9054

Phase I Report

FINITE ELEMENT FORMULATION

A MICROCOMPUTER FINITE ELEMENT SOFTWARE FOR THE DESIGN OF STEEL SUPPORT SYSTEMS WITH SPECIAL REFERENCE TO THE DONKIN MORIEN PROJECT

Submitted by:

Dr. F.P. Hassani

and

Dr. H.S. Mitri

Department of Mining and Metallurgical Engineering

McGill University, Montreal, Quebec, H3A 2A7

Submitted to:

Department of Energy, Mines and Resources

CANMET - CRL Division

Cape Breton Coal Research Laboratory

210 George St.

Sydney, Nova Scotia

B1P 1J3

DSS Contract No: 63 SS. 23440-7-9054-01-SQ

Date: March 1988

60 pp

MICROMEDIA

ABSTRACT

A total Lagrangian, elastic-plastic algorithm for a steel arch model has been developed to examine the strength and stiffness characteristics of mine roadway arch support systems from H-shape steel sections. The six degrees-of-freedom, beam-column element is formulated to simulate the H-section elements and is idealized by three rectangular segments representing the flanges and the web. A twenty-one numerical integration scheme is employed to calculate the tangent stiffness matrix of the element. The material model is trilinear and accounts for yielding, strain hardening and elastic unloading effects. The algorithm for nonlinear stress analysis follows the exact stress-strain model; it checks and corrects any deviation from the material's stress-strain path. The nonlinear analysis is performed by the iterative Newton-Raphson technique which is supplemented with an automatic load increment generator that takes the load to its peak value. In order to ensure the stability of the solution algorithm, a convergence criterion based on incremental energy calculations is invoked to establish and equilibrium configuration in the nonlinear range.

A finite element program called S4 (Steel Set Support Systems) has been written for use on IBM personal computer. The program is coded in standard FORTRAN 77. The required input data for the program is simplified such that only the information related to the physical problem is supplied. Nodal coordinates

and element connectivity arrays, normally required by any conventional finite element program, are automatically generated. This has the advantages of time saving and avoiding human errors. The program's input data include: (1) Problem identification, (2) Support type, (3) Support geometry, (4) Load type and (5) Material properties.

Four support types have been incorporated in S4. These are the circular, semi-circular, semicircular with vertical legs and semicircular with splay legs. Moreover, four loading conditions are accounted for in the program. The user may select: (1) Concentrated gravity load at the crown point, (2) Uniform gravity load over the full length or a portion of the crown, (3) Nonuniform gravity load (peaking at the crown point and decreasing gradually towards the bases) which may be applied over the full length or a portion of the crown and (4) Radial pressure. Furthermore, the user may simulate any arbitrary loading condition. The required material properties are Young's modulus of elasticity and uniaxial yield stress. All input data can be written in free format and the program then runs in batch mode.

The output of program S4 provides complete information on the load-deformation history of the support up to the point of collapse. At any given load level, the corresponding displacements and the extent of yield zones within the support section can be determined. The load is increased automatically

in increments and the results (displacements and stresses) are printed at the end of each load increment. The output is terminated when collapse is imminent and a summary of results is printed. Output of S4 may be stored on a file, routed to the printer, or viewed directly on the personal computer screen.

TABLE OF CONTENTS

ABSTRACT		i
TABLE OF CONTENTS		iv
LIST OF FIGURES AND TABLES		v
NOMENCLATURE		vi
1.	INTRODUCTION	1
2.	FINITE ELEMENT MODEL	6
3.	STRESS ANALYSIS	12
4.	NONLINEAR ANALYSIS	17
5.	AUTOMATIC LOAD CONTROL	18
6.	MODEL SIMULATION	22
7.	ROOF LOAD FORMULAE	30
8.	COMPUTER PROGRAM	35
9.	CONCLUSIONS	49
	REFERENCES	50

LIST OF FIGURES AND TABLES

Fig. 1 : Types of Mine Roadway Steel Supports

Fig. 2 : Beam-Column Element

Fig. 3 : Simulation of H or I - Section

Fig. 4 : Distribution of Numerical Integration Points

Fig. 5 : Material Model

Fig. 6 : Algorithm for Incremental Stress Analysis

Fig. 7 : Automatic Load Control Parameters

Fig. 8 : Support Characteristics Curve

Fig. 9 : Support Model for Convergence Test

Fig. 10 : Results of convergence Tests

Fig. 11 : Discretized Finite Element Models of Steel Supports

Fig. 12 : Sinusoidal Load Distributions

Fig. 13 : A Semicircular Support Under 50% Crown Uniform Load

Fig. 14 : Structure of Program S4

Fig. 15 : Data and Results of Model 1

Fig. 16 : Data and Results of Model 2

Fig. 17 : Data and Results of Model 3

Fig. 18 : Distribution of Yield Zones at Failure for a Semicircular Model under Concentrated Load.

Table 1 : Load Factor Value of Subsequent Load Increments

Table 2 : Properties of H-Sections used as Steel Supports

NOMENCLATURE

a = total depth of section

b = flange width

d = web depth

D = support diameter

E = Young's modulus of elasticity

E_{ij} = current modulus at point ij within the element

E_T = tangent modulus of material model

${}^{n}_{m}E$ = current modulus value after n load increments and m iterations

h = height of vertical or Splay leg

H = support height

L = element length

N_i^K = shape function at node i for degree of freedom K

nel = no. of elements

${}^{1}S$ = slope of load-deflection path in the first load increment

${}^{n}S$ = slope of load-deflection path in the n^{th} load increment

t = flange thickness

u = axial displacement

v = lateral displacement

w = web thickness

W_i, W_j = weight factors

z_j = coordinate in element depth direction

Z = plastic section modulus

Vectors and Matrices

$\mathbf{B}$ = incremental strain-displacement matrix

$\mathbf{B}_L$ = linear strain-displacement matrix

$\mathbf{B}_{NL}$ = nonlinear incremental strain-displacement matrix

$\mathbf{F}$ = element resistance vector

$\mathbf{G}$ = geometric matrix

$\mathbf{K}_{ep}$ = elastic-plastic stiffness matrix

$\mathbf{K}$ = initial stress matrix

$\mathbf{K}_T$ = total tangent stiffness matrix

$\mathbf{P}$ = total external load vector

$\Delta\mathbf{P}$ = incremental load vector

$\mathbf{P}_{el}$ = elastic limit load vector

$\mathbf{R}$ = residual or out-of-balance load vector

$\mathbf{U}$ = nodal displacement vector

$\Delta\mathbf{U}$ = incremental nodal displacement vector

Greek Symbols

α = correction factor for adjusting total stress level

β = load increment factor

γ = tolerence for convergence check

δ = nondimensional percent deformation of support

Δ = crown vertical deflection

ε = normal strain

$\Delta\varepsilon$ = strain increment

ξ = natural coordinate in element length direction

θ = rotational degree of freedom

λ = leg-to-overall height ratio

μ = nondimensional load factor

μ_{ult} = nondimensional load factor at collapse

σ = normal stress

σ_y = yield stress

σ_u = ultimate stress

$\Delta\sigma$ = stress increment

ϕ = splay leg angle

1. INTRODUCTION

The basic requirement of any underground support system is that it controls the movements of the surrounding strata during the period of operation of the tunnel in such a way that the various functions of the tunnel are not impaired. Such functions include: (1) maintaining an opening of sufficient dimensions and (2) holding any loose material in place to ensure the safety of the tunnel. Cambered girders were first used in mine roadways as steel supports but they were eventually replaced by steel arch supports; see Fig. 1. The use of steel arches has resulted in a dramatic reduction of the number of fatalities occurring in mine roadways. Due to their excellent structural performance, the steel arches are now regarded as the most suitable forms of mine tunnel support.

In order to achieve a successful design of a steel support system, information about the roof load and the structural behaviour of the support should be made available. The amount of roof load is determined from the size and the shape of the fractured roof envelope. The latter depends on the rock type, the opening size and the strata condition.

The behaviour of steel supports in mine roadways has been the subject of many investigations carried out over the past two decades. Several methods have been pursued. These included full scale laboratory tests (1,2), full scale underground tests which

were done by either allowing the strata load to develop naturally (3) or by jacking the support into the rock thus simulating its loading (4). Also, physical scale model tests have been done (5). The use of these models is wide spread as they have the advantage of low cost as well as being an exact replica of the full size support. Recently, Hassani et al. (6) suggested two empirically-based formulae to obtain a lower bound estimate of the crown load of steel arches with vertical or splay legs.

Computer-based finite element models have received considerably less attention than other modelling techniques to study the behaviour of steel supports. With the continued advent of powerful digital computers, the potential usefulness of the finite element method in the solution of complex engineering problems has become steadily increasing. In this report, a nonlinear finite element model is developed and used to predict the ultimate strength of steel supports. The problem is one in which the applied (roof) load may induce material yielding and may cause appreciable deformations before the collapse of the arch takes place. Hence, it deemed necessary to incorporate both material and geometric nonlinearities in the present model.

Nonlinear behaviour of frames has been a subject of interest by many researchers. Different methods were proposed to account for the inelastic behaviour due to yielding. For example, Morris and Fenves (7) extended the concept of classical plastic hinge to include the effect of axial forces. Their procedure was based on

modifying the member elastic stiffness matrix and fixed end forces when plastic hinges are formed. A similar approach was invoked in a finite element analysis by Agyris et al. (8) but was extended to include large displacements. A more common approach to evaluate the elastic-plastic stiffness properties of the element is achieved through checking material yielding at certain (sampling) points within the element and then using numerical integration over such points to obtain the tangent stiffness matrix. A variety of integration schemes were suggested. For example, El-Zanaty and Murray (9) used four Gauss quadrature points (2 x 2) whereas Cichon (10) used the Lobatt's five points formula in two directions (5 x 5). Both studies (9,10) employed a 2-node, 8-degrees of freedom beam-column element.

In the present analysis, the beam-column (cubic-linear) element with 6 degrees-of-freedom is utilised; see Fig. 2. The concept of numerical integration is further used; however a new numerical integration scheme is suggested for the evaluation of elastic-plastic stiffness matrix of the element. In order to account for the large deformation effect, a total Lagrangian approach is employed (11). A trilinear material model is also included to account for material nonlinearities due to yielding and strain hardening. The nonlinear analysis is performed using the Newton-Raphson method and is automated to the point of peak load with the help of a load-controller algorithm to be described here.

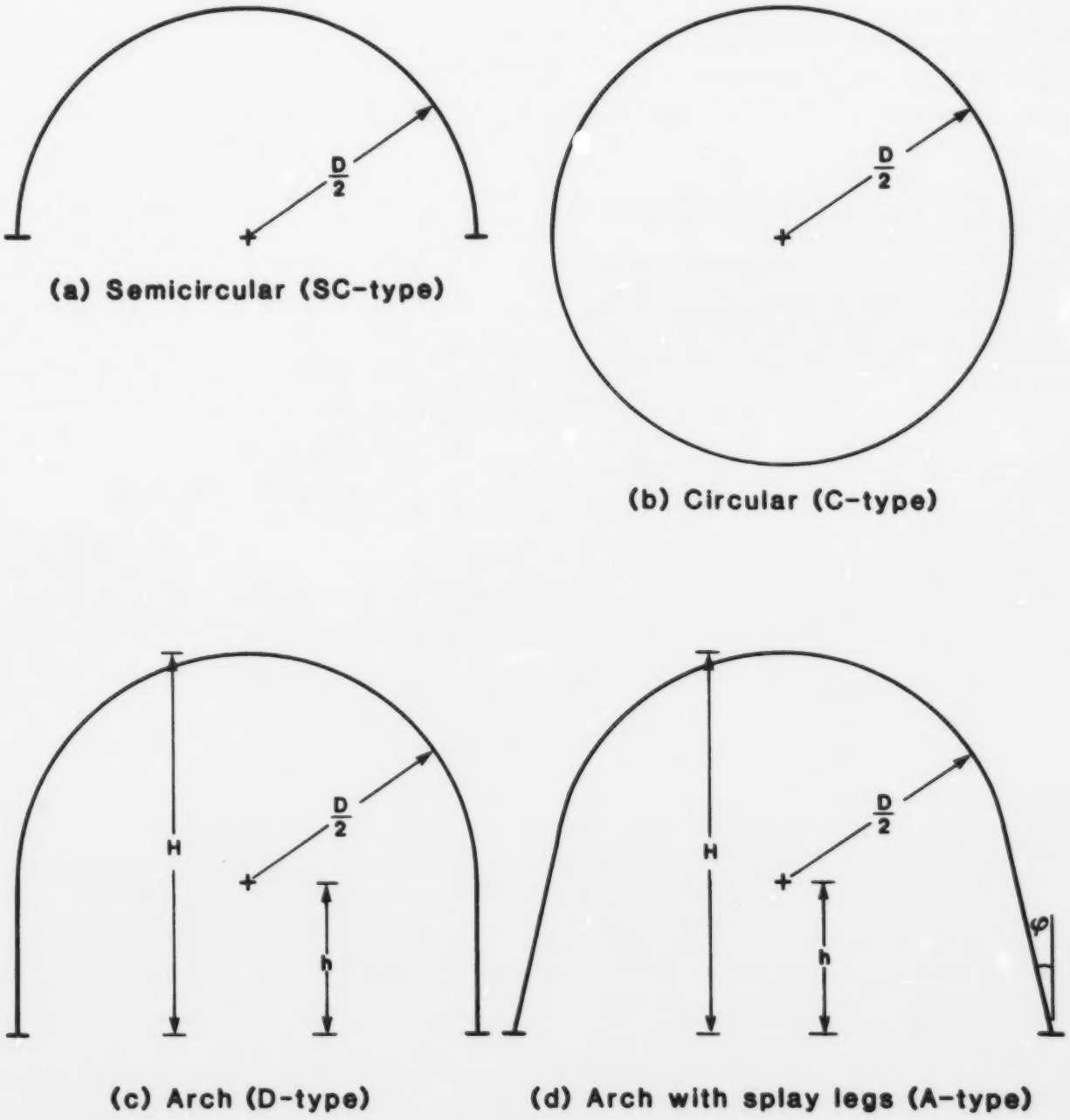

Fig. 1 Types of Mine Roadway Steel Supports

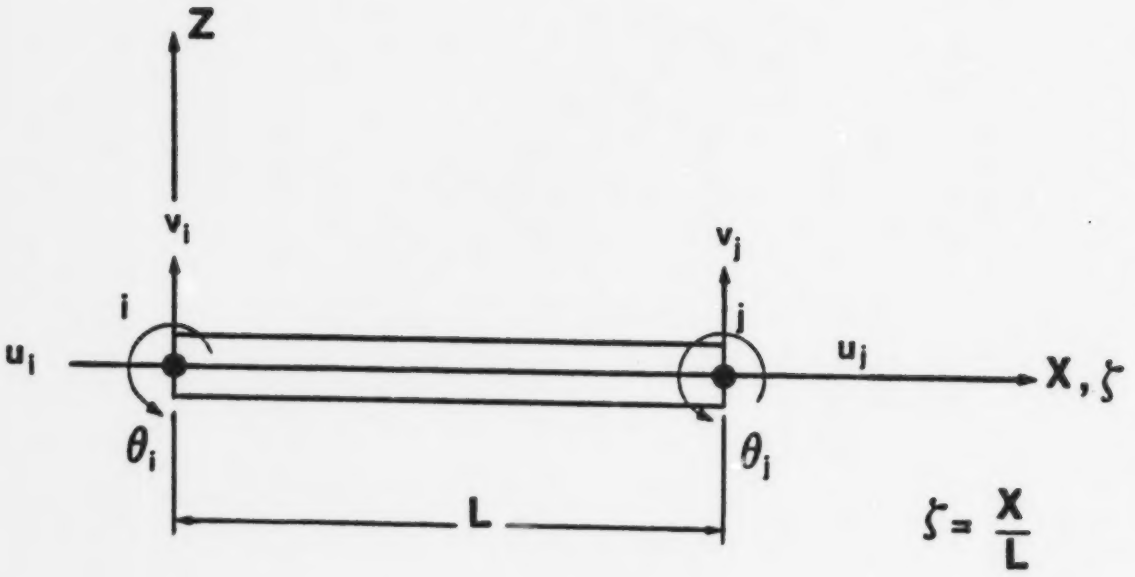

Fig. 2 Beam-Column Element

2. FINITE ELEMENT MODEL

2.1 Strain-Displacement Relation

In its conventional form, Green-Lagrange strain is given by (11)

$$\Delta\varepsilon = \frac{du}{dx} + \frac{1}{2}\left[\left(\frac{du}{dx}\right)^2 + \left(\frac{dv}{dx}\right)^2\right] \tag{1}$$

For a total Lagrangian formulation, equation (1) can be written in matrix, incremental form as follows.

$$\Delta\varepsilon = \mathbf{B} \cdot \Delta\mathbf{U} = (\mathbf{B}_L + \mathbf{B}_{NL}).\Delta\mathbf{U} \tag{2}$$

which relates the incremental strain $\Delta\varepsilon$ to the incremental nodal displacements and rotations $\Delta\mathbf{U}$. The latter is defined as

$$\Delta\mathbf{U}^T = (\Delta u_1,\ \Delta v_1,\ \Delta\theta_1,\ \Delta u_2,\ \Delta v_2,\ \Delta\theta_2) \tag{3}$$

The element strain matrices $\mathbf{B}_L$ and $\mathbf{B}_{NL}$ depend on its assumed shape functions. Based on a linear function for the axial displacement and a cubic function for the lateral displacement, it can be shown that the resulting shape functions of the element are:

$$\begin{aligned}
N_1^u &= 1 - \xi\ , \quad N_2^u = \xi\ , \\
N_1^v &= 1 - 3\ \xi^2 + 2\ \xi^3, \\
N_2^v &= 3\ \xi^2 - 2\ \xi^3, \\
N_1^\theta &= L\ (\xi - 2\ \xi^2 + \xi^3), \\
N_2^\theta &= L\ (\xi^3 - \xi^2)
\end{aligned} \tag{4}$$

Hence, the expressions for the strain-displacement matrices can

be obtained. These are:

$$B_L = B_L(\xi_i, z_j) = [\frac{-1}{L}, \frac{6}{L^2} z_j(1-2\xi_i), \frac{2}{L} z_j(2-3\xi_i), \frac{1}{L},$$

$$\frac{-6}{L^2} z_j(1-2\xi_i), \frac{2}{L} z_j(1-3\xi_i)] \qquad (5)$$

and

$$B_{NL} = B_{NL}(\xi_i) = U^T \cdot G^T \cdot G \qquad (6)$$

which is defined later in equation (15).

2.2 Element Stiffness Matrix

Assuming that the cross section is symmetric about both axes and that it is made of three rectangular segments which may have two different widths b and w, and two different thicknesses t and d, as shown in Fig. 3, it is possible to simulate sections like H or I. The suggested distribution of numerical integration points is shown in Fig. 4; 3 Gaussian stations along the element length and 3 Newton-Cotes points per segment across the depth. The Newton-Cotes points at each Gaussian location yield a total of 7 points due to the overlapping at interfaces of segments and hence the total number of points is 21. This numerical integration scheme is believed to be efficient; it captures the point of initial yield at the extreme fibres of the section when bending action is predominant (a likely occurrence in frame analyses),

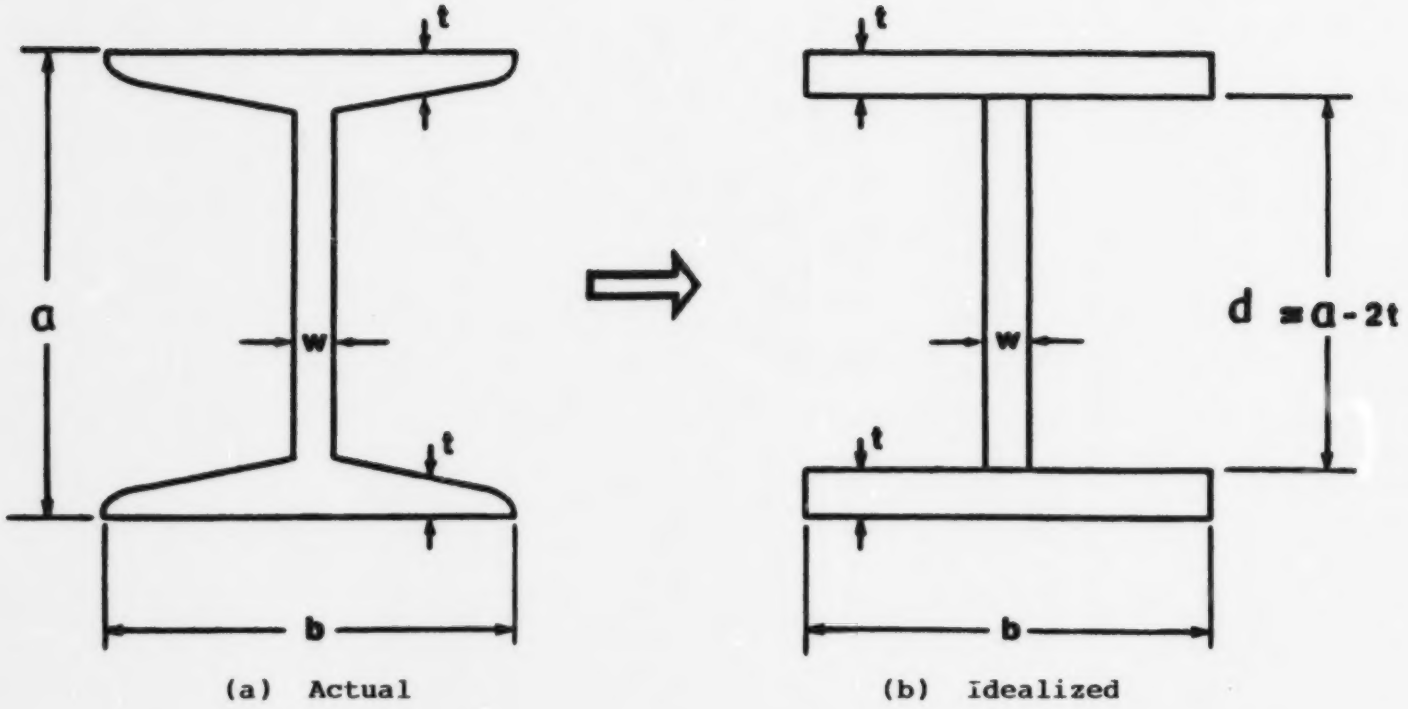

(a) Actual (b) Idealized

Fig. 3 Simulation of H or I - Section

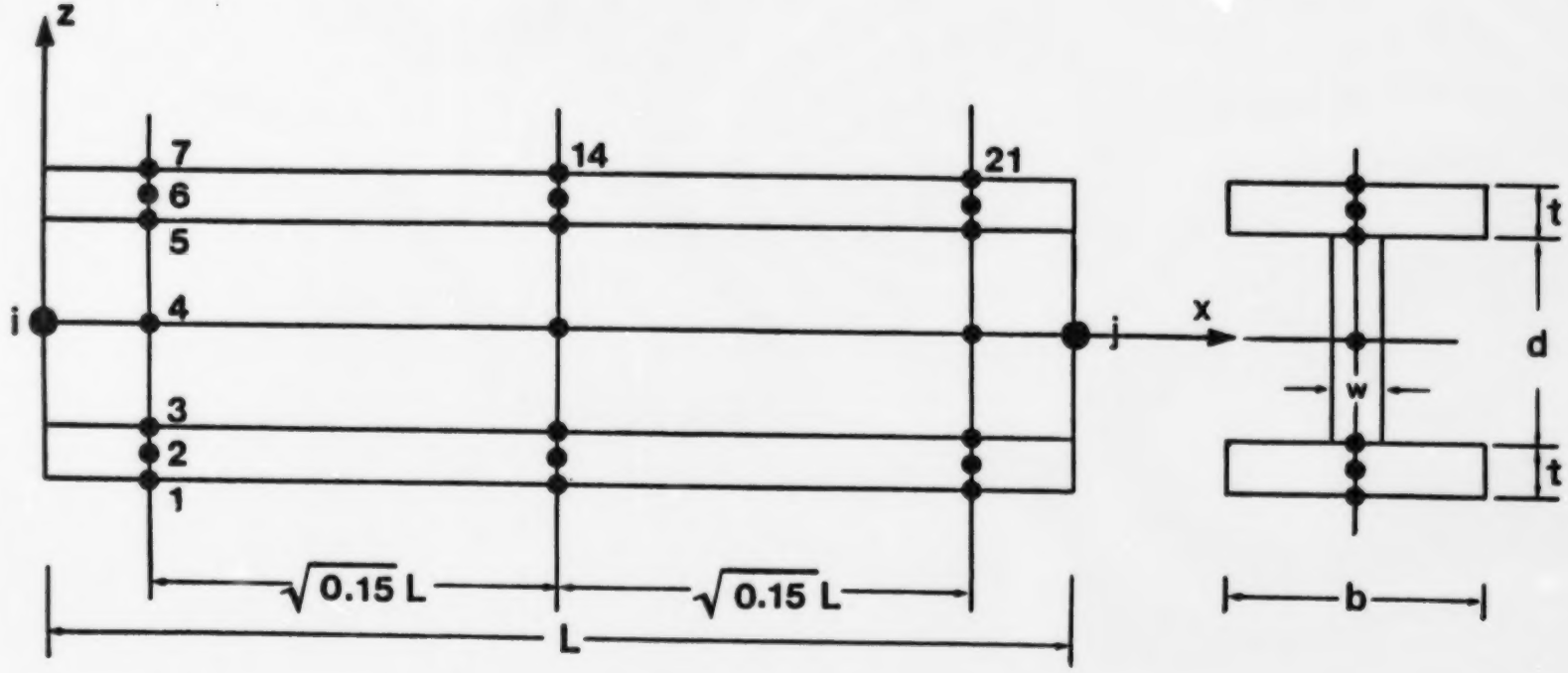

Fig. 4 Distribution of Numerical Integration Points

and it permits material yielding to penetrate through the thickness and to spread over the element length as well. The elastic-plastic stiffness matrix of the element is computed by summing up the stiffness contributions at the 21 sampling points, i.e.

$$\mathbf{K}_{ep} = \int_V \mathbf{B}^T.\mathbf{E}.\mathbf{B}.dV$$

$$= \frac{L}{2} \cdot b \cdot t \sum_{i=1}^{3} \sum_{j=1}^{3} W_i W_j \cdot \mathbf{B}(\xi_i, z_j)^T \cdot E_{ij} \cdot \mathbf{B}(\xi_i, z_j) +$$

$$\frac{L}{2} \cdot w \cdot d \sum_{i=1}^{3} \sum_{j=3}^{5} W_i W_j \cdot \mathbf{B}(\xi_i, z_j)^T \cdot E_{ij} \cdot \mathbf{B}(\xi_i, z_j) +$$

$$\frac{L}{2} \cdot b \cdot t \sum_{i=1}^{3} \sum_{j=5}^{7} W_i W_j \cdot \mathbf{B}(\xi_i, z_j)^T \cdot E_{ij} \cdot \mathbf{B}(\xi_i, z_j) \qquad (7)$$

where

$$W_i = (5/9,\ 8/9,\ 5/9) \qquad (8)$$

and

$$\xi_i = (0.5 - \sqrt{0.15},\ 0.5,\ 0.5 + \sqrt{0.15}) \qquad (9)$$

are the weight factors and the natural co-ordinates of Gauss points respectively. The respective quantities for Newton-Cotes points are:

$$W_j = (1/6,\ 4/6,\ 1/6,\ 4/6,\ 1/6,\ 4/6,\ 1/6) \qquad (10)$$

$$z_j = ((-d/2-t),\ (-d/2-t/2),\ (-d/2),\ (0.0),\ (d/2),\ (d/2+t/2),\ (d/2+t)) \qquad (11)$$

If b = w and t = d, equation (7) reduces to a beam-column element with solid rectangular cross section whereby the sampling points across the depth will be evenly spaced and

$$\mathbf{K}_{ep} = b \frac{L}{2} t \sum_{i=1}^{3} \sum_{j=1}^{7} W_i . W_j . \mathbf{B}(\xi_i, z_j)^T . E_{ij} . \mathbf{B}(\xi_i, z_j) \qquad (12)$$

In this case,

$$W_j = (1/6,\ 4/6,\ 2/6,\ 4/6,\ 2/6,\ 4/6,\ 1/6) \qquad (13)$$

In equation (7), $\mathbf{B}(\xi_i, z_j)$ is the total incremental strain-displacement matrix at a point including Green-Lagrange nonlinear strain component due to large displacements (11). Also in equation 7, E_{ij} is the tangent modulus which depends on the stress level. This will be further explained later. The initial stress matrix $\mathbf{K}$ is a function of the total stress σ_{ij} and it can be calculated by numerical integration as follows.

$$\mathbf{K} = \int_V \mathbf{G}^T . \sigma . \mathbf{G}\, dV$$

$$= \frac{L}{2} \sum_{i=1}^{3} W_i . \mathbf{G}(\xi_i)^T . \mathbf{G}(\xi_i) \left[bt \sum_{j=1}^{3} \sigma_{ij} . W_j + wd \sum_{j=3}^{5} \sigma_{ij} . W_j + bt \sum_{j=5}^{7} \sigma_{ij} . W_j \right] .... \qquad (14)$$

where $G(\xi_i)$ is the element geometric matrix and is a function of the coordinate . This is defined as follows.

$$G = \begin{bmatrix} \frac{dN_1^u}{dx} & 0 & 0 & \frac{dN_2^u}{dx} & 0 & 0 \\ 0 & \frac{dN_1^v}{dx} & \frac{dN_1^\theta}{dx} & 0 & \frac{dN_2^v}{dx} & \frac{dN_2^\theta}{dx} \end{bmatrix} \quad \ldots (15)$$

Substituting for the shape functions from equation (4) and differentiating with respect to x yields

$$G = G(\xi_i) = \begin{bmatrix} -1/L & 0 & 0 & 1/L & 0 & 0 \\ 0 & \frac{6}{L}(\xi_i+\xi_i^2) & 1-4\xi_i+3\xi_i^2 & 0 & \frac{6}{L}(\xi_i-\xi_i^2) & 3\xi_i^2-2\xi_i \end{bmatrix} \quad (16)$$

Also, in (14), σ is a diagonal normal stress matrix and is 2 x 2.

The total tangent stiffness matrix is then given by:

$$K_T = K_{ep} + K_\tau \quad (17)$$

3. STRESS ANALYSIS

An elastic-plastic material with strain hardening is assumed. The stress-strain relation is shown in Fig. 5. The material is described by the Young's modulus of elasticity E, the yield stress σ_y, the tangent modulus E_T and the ultimate stress

σ_u. If unloading is detected, the stress drops linearly with a slope equal to E to account for the elastic behaviour of unloading. Also, if the normal stress reaches the ultimate stress value, no further strain hardening is allowed.

When the material is within the elastic range, the stress increment at any point can be calculated from

$$\Delta\sigma = E \cdot \Delta\varepsilon \tag{18}$$

In the above, $\Delta\varepsilon$ is to be first calculated from equation (2). In the post-elastic range, stresses and strains are also calculated incrementally. In this case the following stress-strain relation replaces equation (18).

$$\overset{n}{\underset{m}{\Delta\sigma}} = \overset{n}{\underset{m-1}{E}} \cdot \overset{n}{\underset{m}{\Delta\varepsilon}} \tag{19}$$

Generally, the total stress would then be given by

$$\overset{n}{\underset{m}{\sigma}} = \overset{n}{\underset{m-1}{\sigma}} + \overset{n}{\underset{m}{\Delta\sigma}} \tag{20}$$

The algorithm implemented in the model is based on the general procedure suggested by Owen and Hinton (12). It accounts for five possibilities that may occur in the elastic-plastic range. Comparing the yield stress and the ultimate stress with the total new stress σ^N and the total stress from previous iteration σ^P, during the m^{th} iteration, it can be demonstrated

that one of the following situations must exist (Fig. 6). These are:

1. The stress is still within the elastic range ($^{n}_{m}E = E$)
2. The stress was elastic and is now in the plastic range ($^{n}_{m}E = E_T$)
3. The stress was and still is in the plastic range ($^{n}_{m}E = E_T$)
4. The stress was in the plastic range and has now exceeded the ultimate stress ($^{n}_{m}E = 0$)
5. The stress is decreasing indicating material unloading ($^{n}_{m}E = E$)

The second situation, representing elastic-to-plastic transition often requires a correction of total stress level, $^{n}_{m}\sigma$, in order to prevent possible deviation from the stress-strain path of the material. The corrected stress level is given by

$$^{n}_{m}\sigma = {}^{n}_{m-1}\sigma + {}^{n}_{m}\Delta\sigma \cdot \alpha + (1-\alpha)\, E_T \cdot {}^{n}_{m}\Delta\sigma \qquad (21)$$

where $\alpha = (\sigma_y - \sigma^P)/{}^{n}_{m}\Delta\sigma$, is the correction factor.

The term $^{n}_{m}\Delta\sigma \cdot \alpha$ represents the elastic stress increment whereas $(1-\alpha)\, E_T \cdot {}^{n}_{m}\Delta\varepsilon$ represents a stress increment in the plastic range.

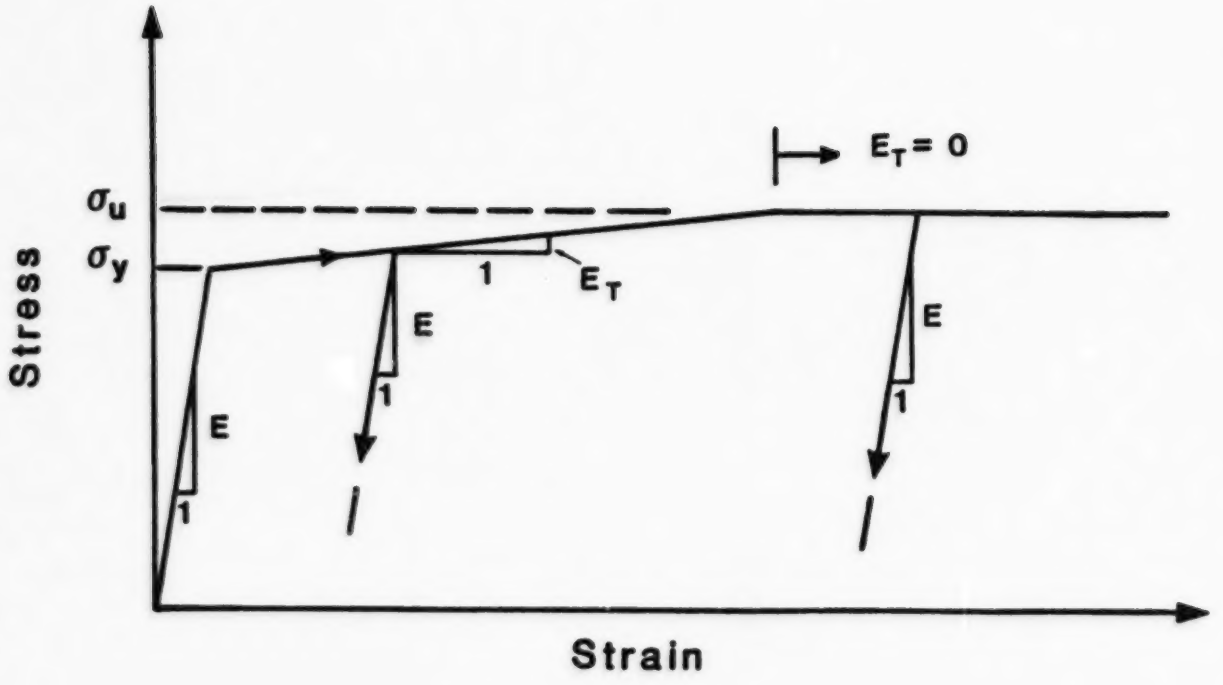

Fig. 5 Material Model

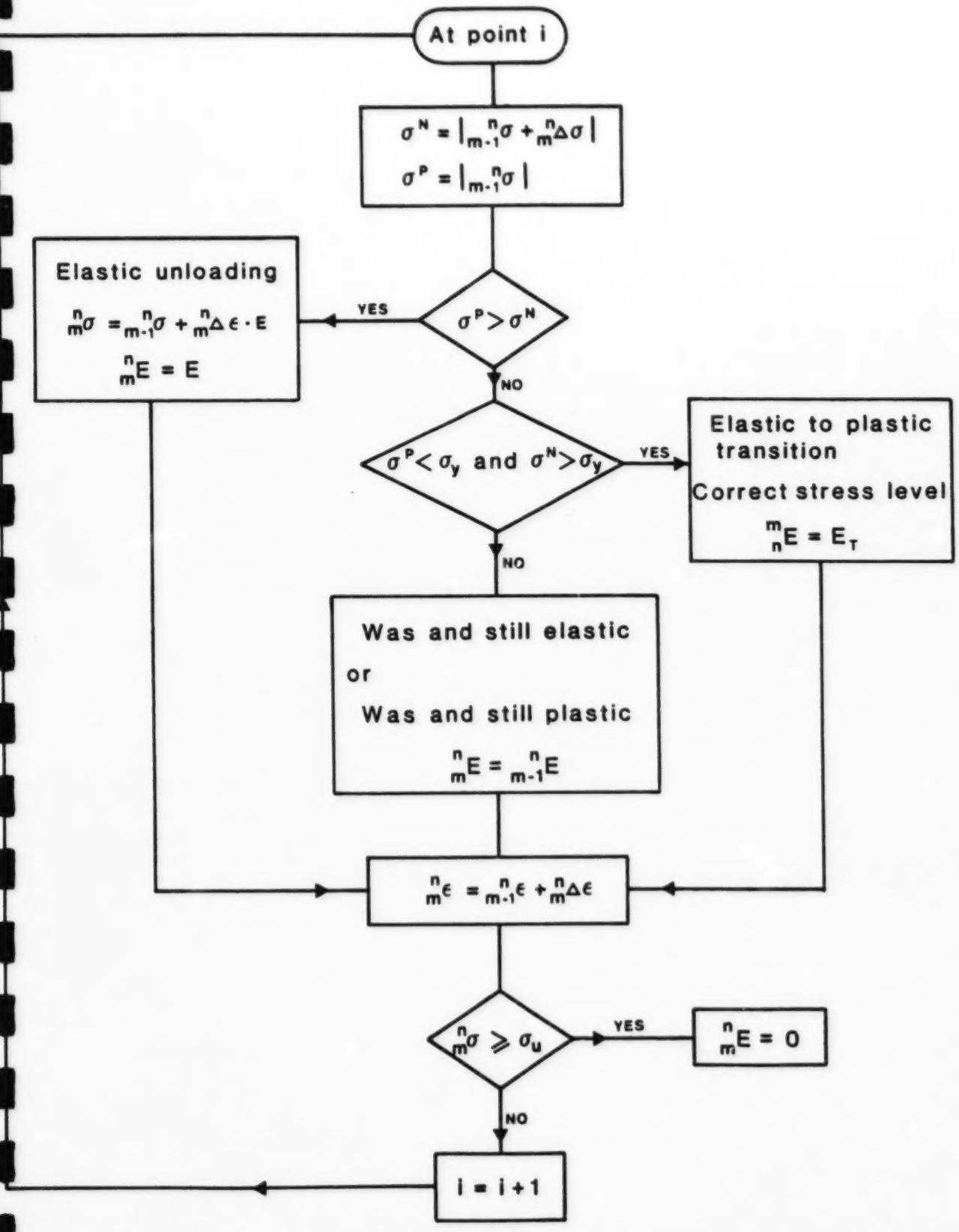

Fig. 6 Algorithm for Incremental Stress Analysis

4. NONLINEAR ANALYSIS

The global incremental equations of equilibrium are established using the principle of virtual incremental displacements (10). These are solved iteratively for the incremental displacements, strains and stresses. The nonlinear analysis is carried out by the conventional Newton-Raphson technique, i.e. the global stiffness matrix ${}^{n}_{m}\mathbf{K}_T$ is updated and the out-of-balance force vector ${}^{n}_{m}\mathbf{R}$ is computed after each iteration m in the n^{th} load increment. The out-of-balance forces ${}^{n}_{m}\mathbf{R}$ are calculated as the difference between the total external load ${}^{n}\mathbf{P}$ and the total resistance offered by the structure ${}^{n}_{m}\mathbf{F}$, i.e.

$$ {}^{n}_{m}\mathbf{R} = {}^{n}\mathbf{P} - {}^{n}_{m}\mathbf{F} \tag{22} $$

$$ \text{where } {}^{n}_{m}\mathbf{F} = \sum_{i=1}^{nel} \int_{v} \mathbf{B}^T \cdot {}^{n}_{m} \, dV \tag{23} $$

Having evaluated ${}^{n}_{m}\mathbf{R}$, the system of equilibrium equations can be solved for the incremental displacements ${}^{n}_{m}\Delta\mathbf{U}$ as follows

$$ {}^{n}_{m}\mathbf{R} = {}^{n}_{m}\mathbf{K}_T \cdot {}^{n}_{m}\Delta\mathbf{U} \tag{24} $$

Knowing ${}^{n}_{m}\Delta\mathbf{U}$ enables the calculation of strains and stresses within the elements and hence new tangent stiffness matrices can be obtained and equation (24) can be solved again for another set of incremental displacements at the nodes. This procedure is

repeated until there is sufficient evidence that convergence to an equilibrium state between the applied load and the support resistance exists.

Convergence of the iterations is checked using an energy convergence criterion (13). The work done by the out-of-balance forces in the m^{th} iteration through the incremental displacements ${}^{n}_{m}\Delta U$ is compared with the initial internal energy increment in the first iteration. The ratio between the two quantities, γ, serves as a convergence measure. Typically, when $\gamma \leq 0.001$, the iteration is terminated. Thus, convergence takes place when

$$\gamma = \frac{{}^{n}_{m}R^{T} \cdot {}^{n}_{m}\Delta U}{{}^{n}_{1}R^{T} \cdot {}^{n}_{1}\Delta U} \leq 0.001 \qquad (25)$$

5. AUTOMATIC LOAD CONTROL

Bathe and Dvorkin (14) suggested an algorithm for the automatic incremental solution of nonlinear problems. Their algorithm, designed for snapping problems, is a combination of Riks' (15) spherical arc length technique and the constant external work method. In order to successfully implement their algorithm, the user must specify a priori a nodal displacement corresponding to the first load level and the maximum size of the load-deflection step. Both of these parameters are problem dependent. In the present analysis, the primary objective was to develop a model for the prediction of ultimate strength and

therefore, a snap-through algorithm was not called for. Moreover, an algorithm for automatic generation of load increments was required to facilitate the use of the model. The method devised is semi-empirical; it is based on the authors' numerical experience and does not require user-input parameters.

Firstly, the elastic limit load vector $\mathbf{P}_{el}$ is calculated assuming a small displacement response, and 20% of this is taken as the first load increment of the nonlinear analysis. Thus

$$^{1}\Delta\mathbf{P} = 0.20\ \mathbf{P}_{el} \tag{26}$$

Subsequent load increments $^{n}\Delta\mathbf{P}$ are given by

$$^{n}\Delta\mathbf{P} = {}^{n}\beta\ .\ {}^{1}\Delta\mathbf{P} \tag{27}$$

where $^{n}\beta \leq 1$. The criteria for selecting $^{n}\beta$ are explained as follows.

1. At the end of the first load increment, calculate the norms of the load increment $\|^{1}\Delta\mathbf{P}\|$ and the total displacement vector $\|^{1}\mathbf{U}\|$, then define

$$^{1}S = \|^{1}\Delta\mathbf{P}\| \,/\, \|^{1}\mathbf{U}\| \tag{28}$$

As can be seen from Fig. 7, ^{1}S represents the slope of load-deflection path in one-dimensional space, at an early stage of the loading when the structure is stiffest.

2. Having reached convergence at the end of load increment n, calculate the respective quantities ${}^{n}_{\Delta P}$, ${}^{n}_{\Delta U}$ and ${}^{n}S$, where in this case,

$$ {}^{n}_{\Delta U} = {}^{n}U - {}^{n-1}U \tag{29} $$

3. Calculate the ratio ${}^{n}S/{}^{1}S$, this is a measure of the stiffness deterioration in the structure. From numerical experience, a set of values for ${}^{n+1}\beta$ corresponding to ${}^{n}S/{}^{1}S$ ratios have been established. Such values are listed in Table 1. It may be observed from the Table that as ${}^{n}S/{}^{1}S$ decreases (indicating increased plasticity) ${}^{n+1}\beta$ also decreases. The actual load increment to the next load level is then computed as

$$ {}^{n+1}\Delta P = {}^{n+1}\beta \cdot {}^{1}\Delta P + {}^{n}R \tag{30} $$

in which ${}^{n}R$ is the residual load vector from the last (converged) iteration in previous load increment and is calculated from equation (19).

Table 1 Load Factor Value of Subsequent Load Increments

${}^{n}S/{}^{1}S$	>0.9	>0.8 to 0.9	>0.7 to 0.8	>0.6 to 0.7	<0.6
${}^{n+1}\beta$	1.0	0.8	0.6	0.4	0.2

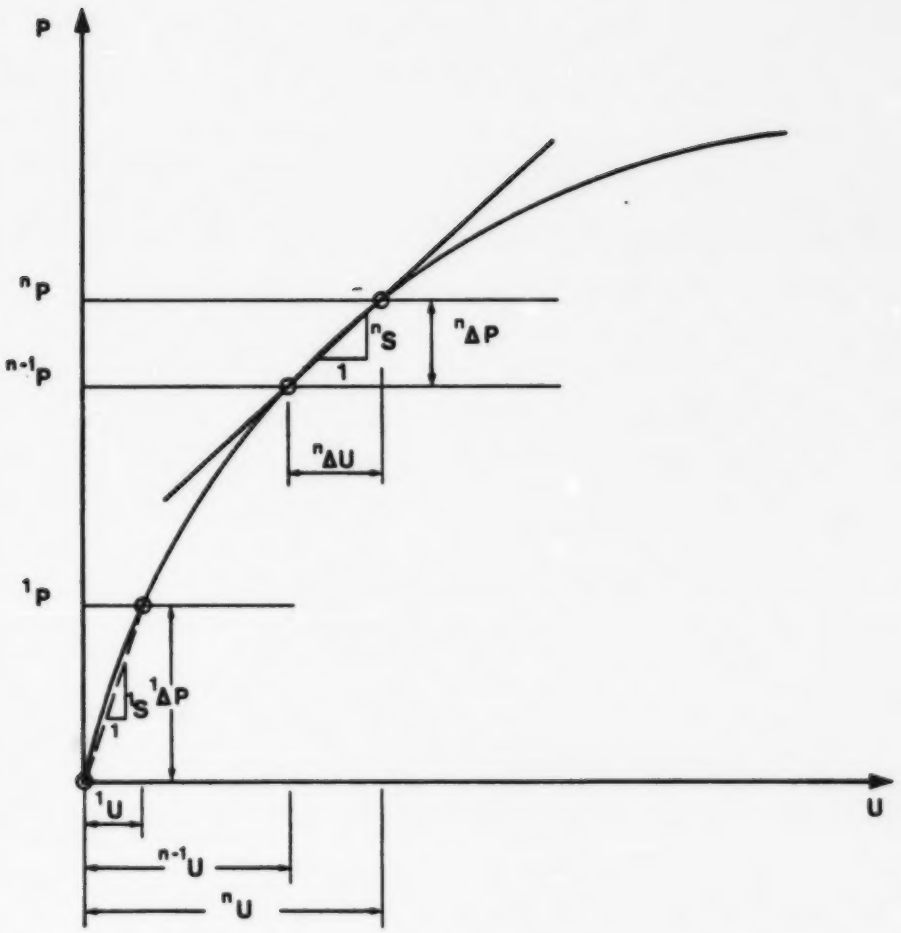

Fig. 7 Automatic Load Control Parameters

6. MODEL SIMULATION

The support geometry is defined by three basic parameters; the arch diameter D, the leg-to-overall height ratio $\lambda = h/H$ and the splay leg angle ϕ indicated in Fig. 1. The support characteristics are determined from its load-deflection curve illustrated in Fig. 8, whereby the load represents either a concentrated force acting at the crown point or the sum of distributed loads applied over a portion of or the whole crown length. The deformational response, δ, is expressed in terms of a percentage of the crown vertical deflection, Δ, to the support diameter, D, i.e.

$$\delta = \frac{\Delta}{D} \times 100 \tag{31}$$

Only half of the support need be considered for the finite element simulation because of symmetry of both geometry and loading. In order to determine the appropriate number of elements required for the finite element discretization, a convergence test seemed necessary. This was done using a semi-circular steel model which was subjected to an incremental, concentrated load applied at the crown as shown in Fig. 9. The total number of elements used was varied from 10 to 18. The collapse load was recorded an plotted against the number of elements selected in each case. As can be seen from Fig. 10, the ultimate strength practically ceases to change as the number of

elements is increased from 16 to 18. Thus, SC-type support is discretized into 18 elements of equal length (Fig. 11a). For the D-type model, the vertical leg is subdivided into 6 elements resulting in a total of 24 elements (Fig. 11b). Similarly, the A-type model used 24 elements as indicated in Fig. 11c. All three models are assumed to be pinned at the base. For the circular support model, only a quadrant is considered when the support is subjected to radial pressure and hence 18 elements are used. In this case, the boundary constraints take the form of guided rollers as shown in Fig. 11d. In case of gravity-type loads, half of the circular model must be simulated. Thus 36 elements are used (Fig. 11e). The bottom end of the support is assumed to be fixed whereas that at the top (under the load) is a guided roller. The steel material of all models is assumed linear elastic-perfectly plastic to allow yielding and hence inelastic deformations to come into place. The support cross-section is an open steel H or I- type.

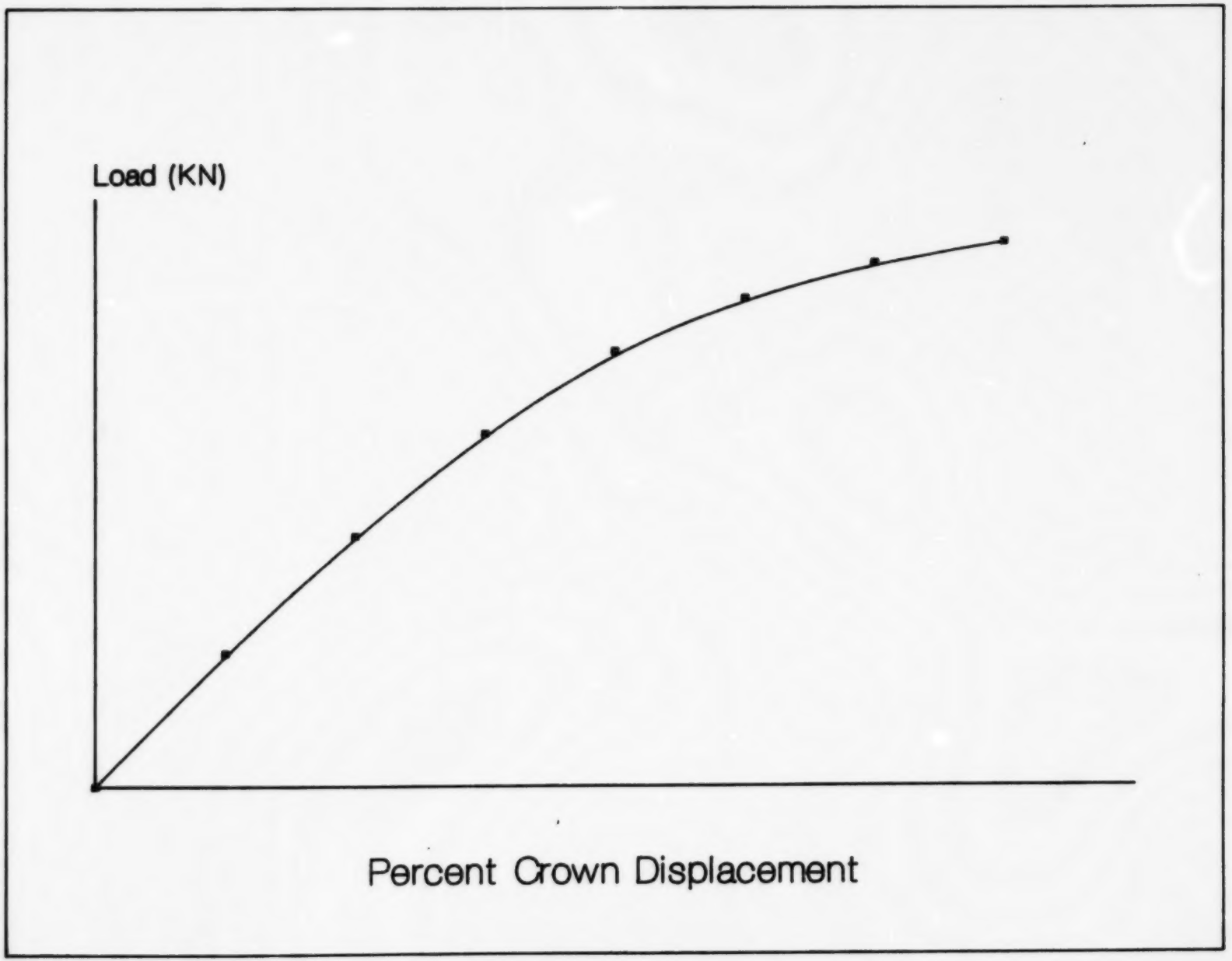

Fig. 8 Support Characteristics Curve

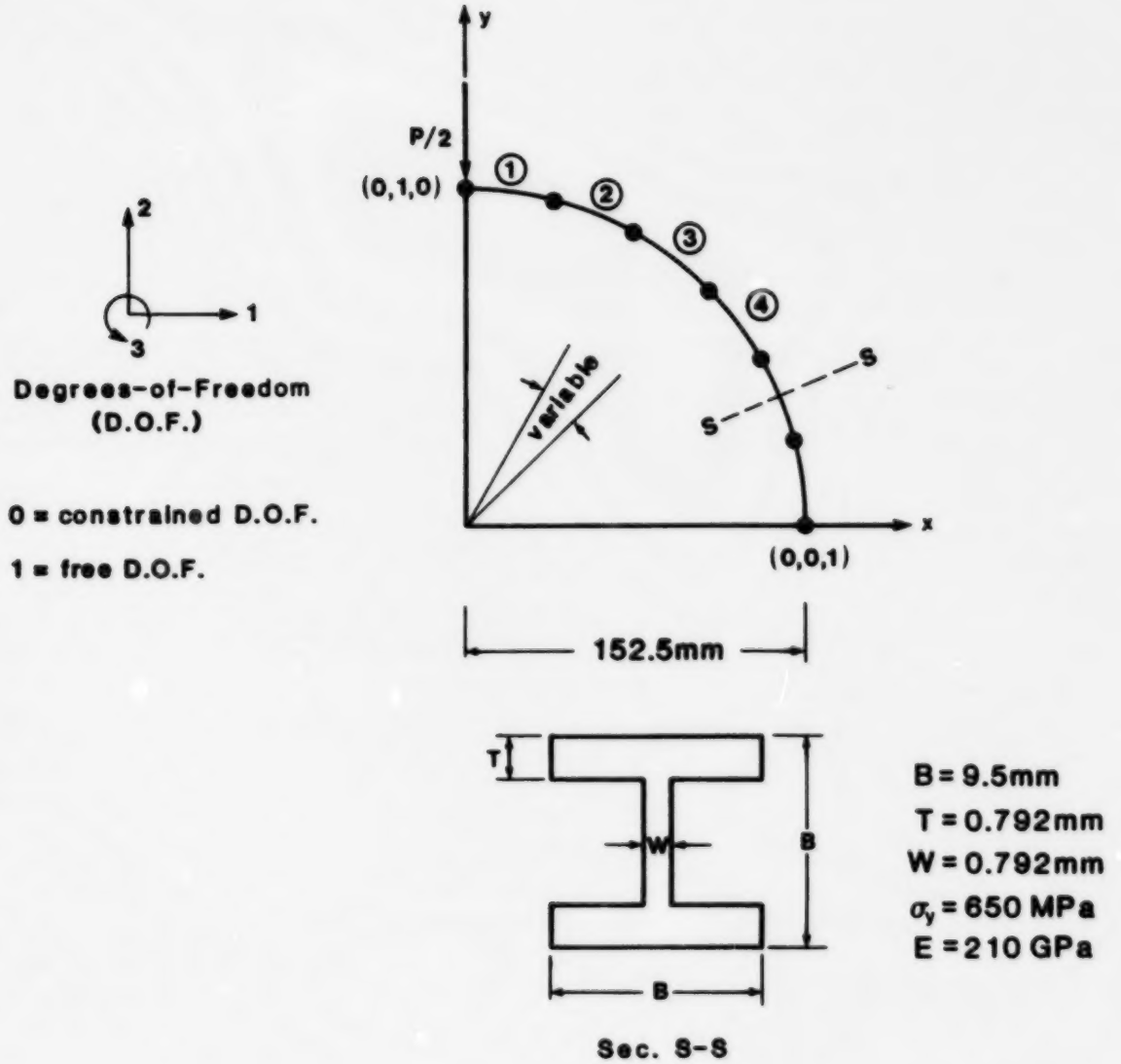

Fig. 9 Support Model for Convergence Test

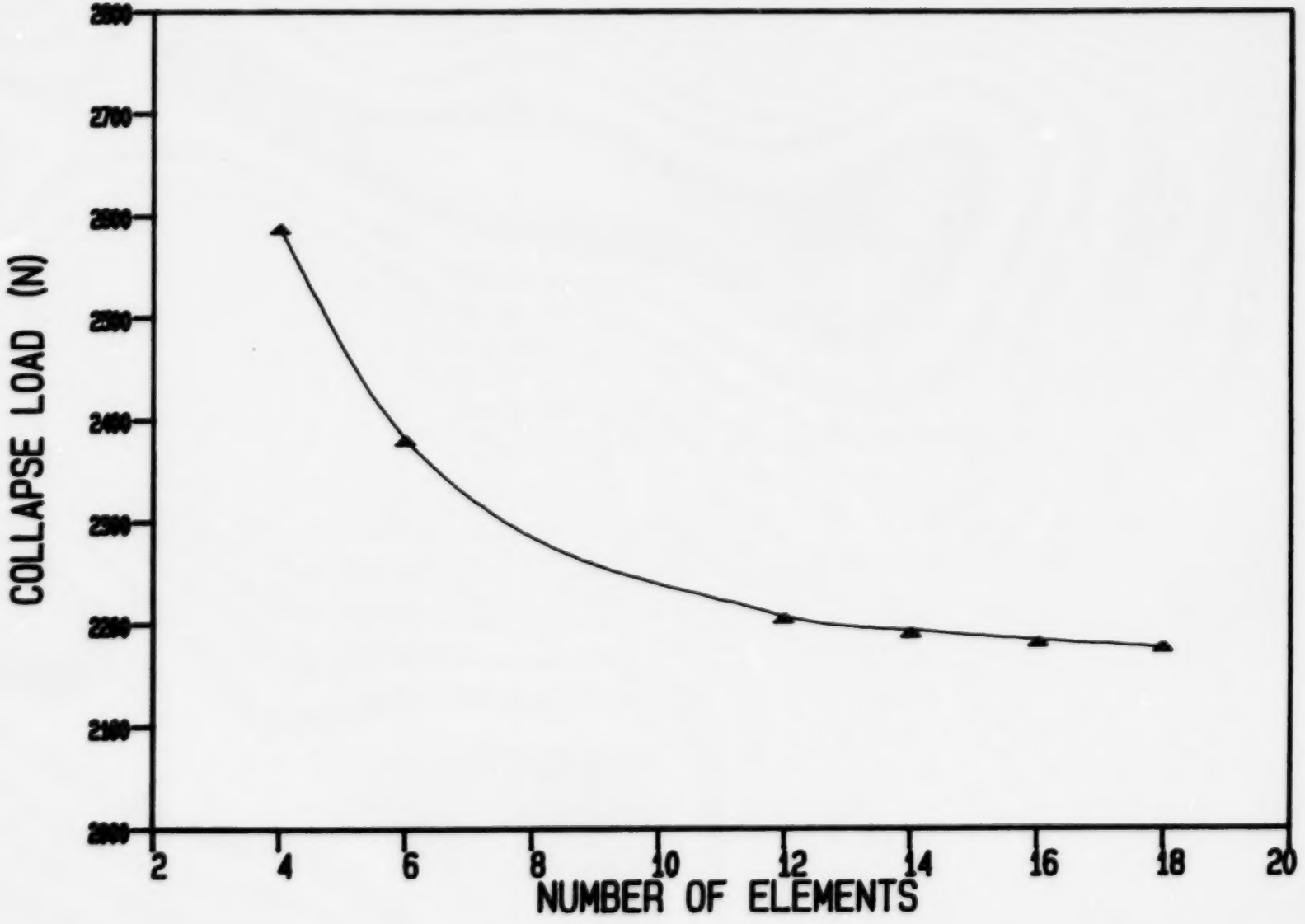

Fig. 10 Results of Convergence Test

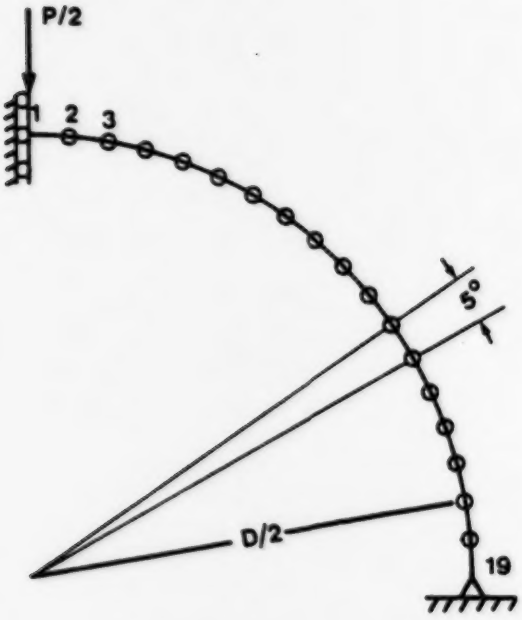

(a) Semicircular

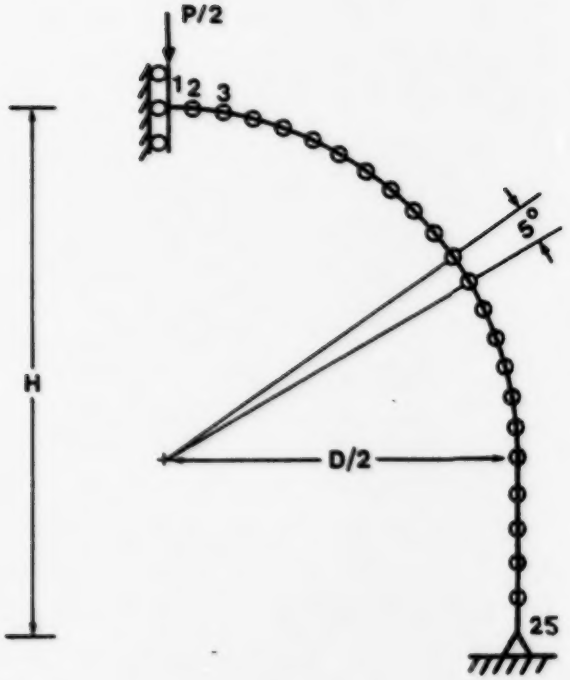

(b) Arch

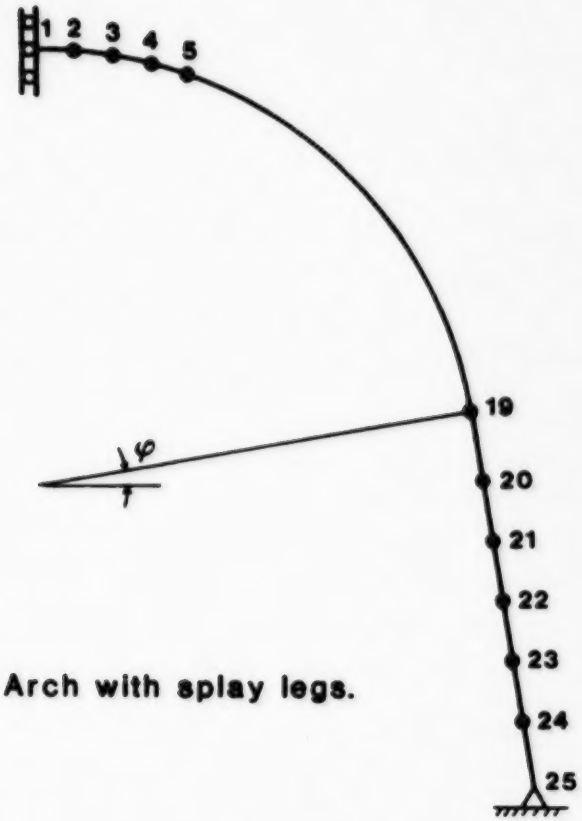

c) Arch with splay legs.

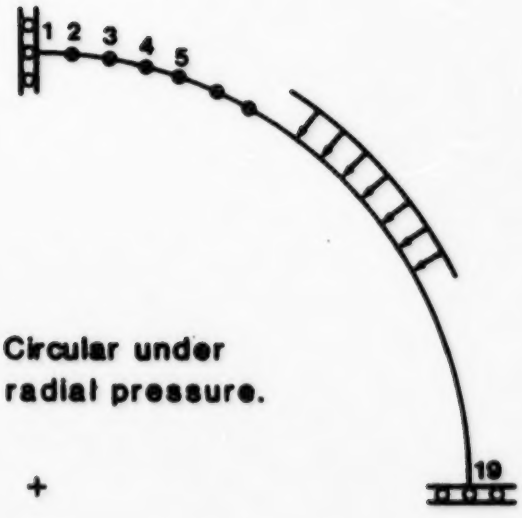

d) Circular under radial pressure.

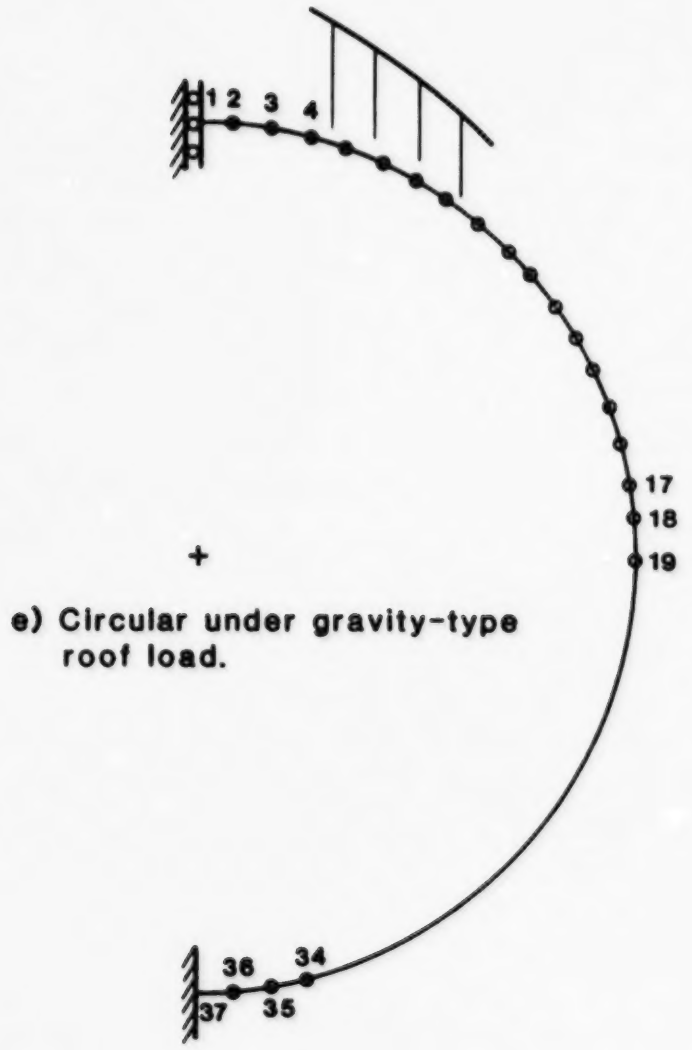

e) Circular under gravity-type roof load.

Fig. 11 Discretized Finite Element Models of Steel Supports

7. ROOF LOAD FORMULAE

The main strata loading consideration which must be accounted for when selecting a steel support is that the latter should offer sufficient resistance to carry the envelope of fractured strata formed above the roadway as a result of the excavation. Instrumentation techniques, developed to measure the extent of fractured zone around the roadway opening indicated the development of a nonuniform gravity-type loading pattern above the steel support (16). A convenient load envelope which conforms with in-situ observation and yet is easy to calculate is the sinusoidal one in which the load per unit length is given by (Fig. 12a):

$$p = \mu \sin\theta \tag{32}$$

where μ = nondimensional load factor; its value is obtained from the results of the numerical model. It can be seen from Fig. 12 that this type of distribution provides a maximum load at the crown point which diminishes gradually to zero at the base. The total gravity load, P_u, is calculated from:

$$P_u = \int_s \mu \sin\theta \, ds \tag{33}$$

Substituting for $ds = \frac{D}{2} d\theta$,

$$P_u = \int_0^{\pi} \mu \frac{D}{2} \sin\theta \, d\theta \tag{34}$$

which after integration gives

$$P_u = \mu D \qquad (35)$$

In case of A-type support, it is assumed that the splay legs will also be subjected to gravity load which is uniform and equal to $p = \mu \sin\phi$ (Fig. 12b). Thus,

$$P_u = \int_{\phi}^{\pi-\phi} \mu \frac{D}{2} \sin\theta \, d\theta + 2 \mu \sin\phi \left(\frac{D}{2} \sin\phi + h\right)/\cos\phi \qquad \ldots (31)$$

which leads to

$$P_u = \mu D + 2 \mu \tan\phi \left(\frac{D}{2} \sin\phi + h\right) \qquad (36)$$

In order to carry out an analysis, an initial value for μ should be assumed. In the model $\mu = 1$ is used as initial value. This will preserve the shapes of all load envelopes just described. The nonlinear analysis is then carried out and μ is increased incrementally as further resistance is offered by the support until plastic failure of the steel support is detected, at which point $\mu = \mu_{ult}$. The latter (μ_{ult}) can then be used in equation (30) or equation (32), depending on the assumed load envelope, to obtain the load-carrying capacity of the support.

Other loading types, that are included in the model are: (1) concentrated load at the crown point, (2) uniformly distributed load and (3) radial pressure. Furthermore, the model

allows for the load application over a portion of the projected crown length. For example, Fig. 13 illustrates a semicircular support subjected to uniform load applied to 50% of the projected crown length.

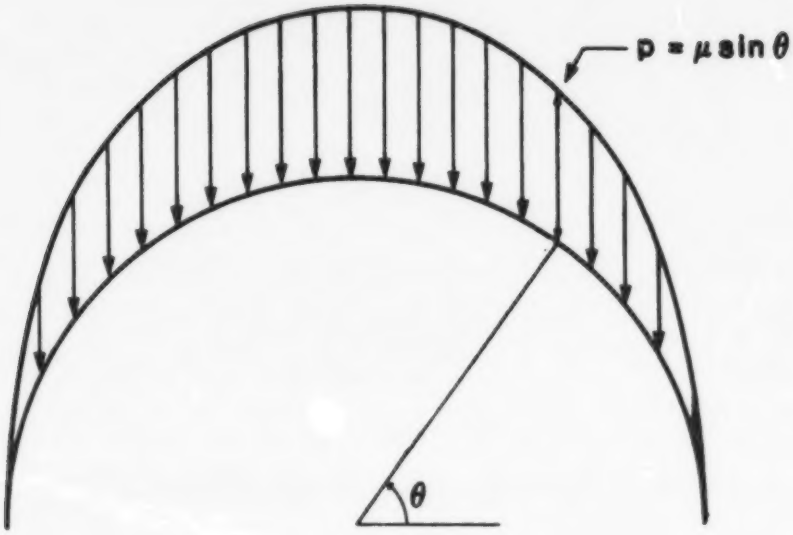

a) SC or D-Type

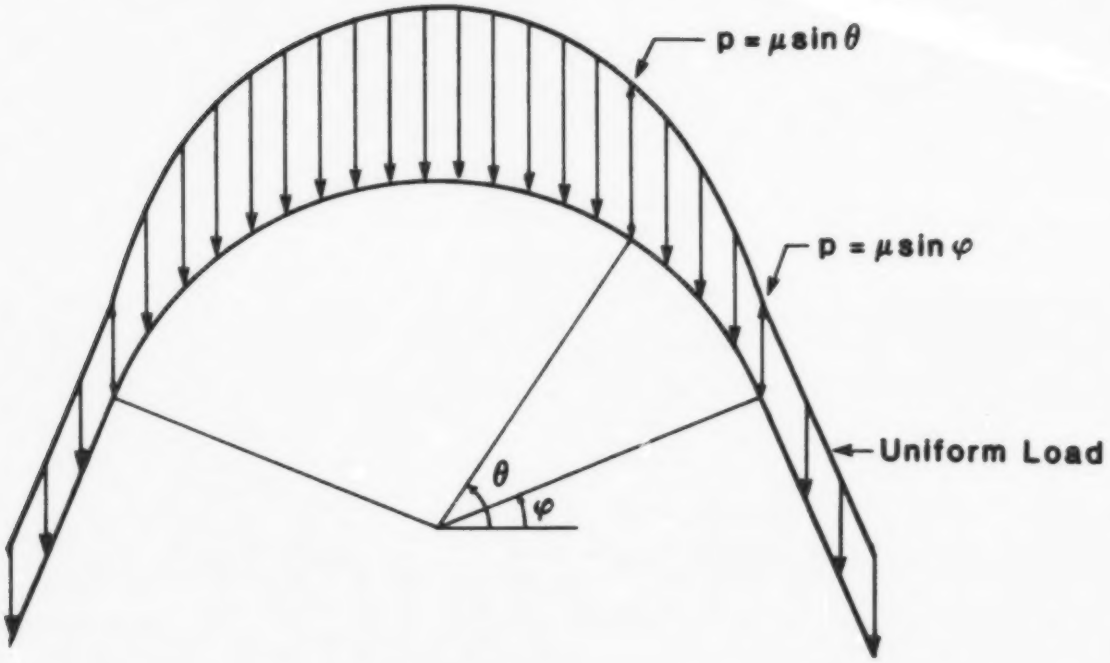

b) A-Type

Fig. 12 Sinusoidal Load Distributions

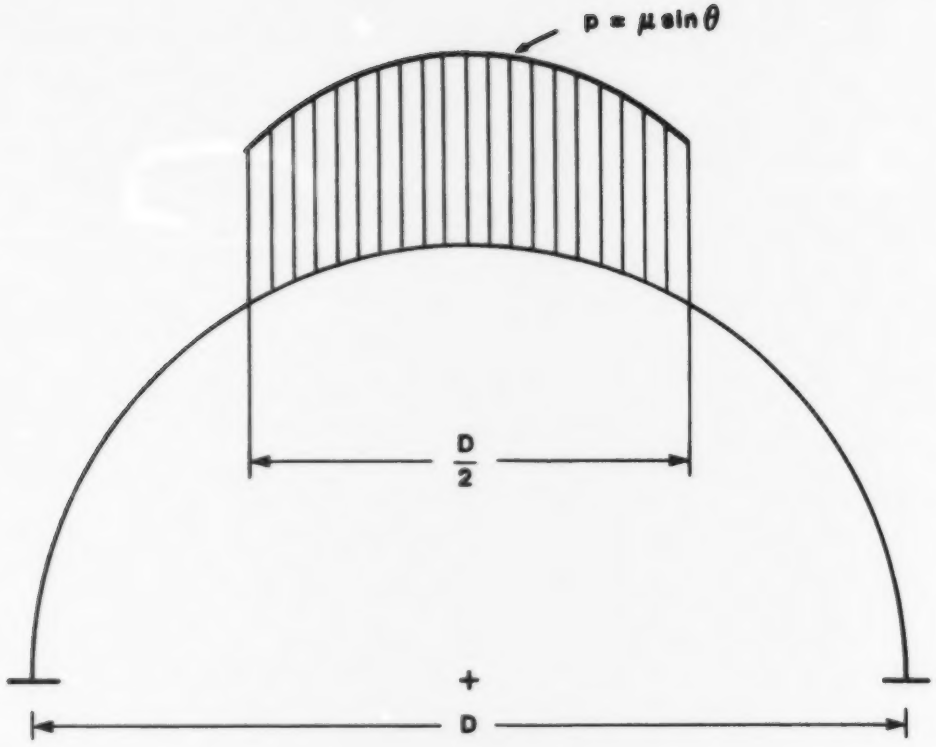

Fig. 13 A Semicircular Support Under 50% Uniform Load

8. COMPUTER PROGRAM

The finite element model just described has been coded in standard FORTRAN 77. The computer program called S4 (Steel Set Support Systems) is tailored for use on microcomputer. Currently, the program runs on IBM and Olivetti personal computers. With the help of the skyline technique in assembling the global stiffness matrix (17) and the dynamic storage allocation in a single array, it has been possible to reduce the memory requirements and fit the program on any IBM-compatible 640 Kb personal computer.

Fig. 14 shows the basic structure of program S4; it consists of a controller and 32 subroutines. A detailed description of the computer program and the user's manual is beyond the scope of this report. This information will be made available in Phase II documentation of this project. For the purpose of illustration, some model results are reported herein. Figures 15 to 18 present the discretized finite element models of a semicircular, arch and splay-leg arch support. All 3 models have a diameter of 4000 mm and utilize an H-section whose geometric and mechanical properties are listed in Table 2 under H3. The leg-to-overall height ratio is 0.4 and the splay leg angle is 10^{o}. Each model is subjected to 3 different loading conditions namely uniformly distributed, sinusoidal and crown concentrated load. The load-deformation (characteristic) curves are plotted in Figures 15c, 16c and

17c for the three models.

Frthermore, in order to demonstrate the failure pattern predicted by the S4 program, the distribution of plastic zones prior to failure is sketched for a semicircular model subject to crown concentrated load in Fig. 18. It suggests that the failure mechanism is due to plastic instability; it comprises a plastic hinge at the crown (elements Nos. 1 and 2) and excessive yielding along the shoulder at angles of 20^{o} - 50^{o} with the horizontal (elements Nos. 9-14). The unsymmetric pattern of yield zones about the centroidal axis is due to the compressive membrane stress which, when coupled with bending action at the shoulder, induces more yielding on the inner flange of the H-section and relieves stress on the other one.

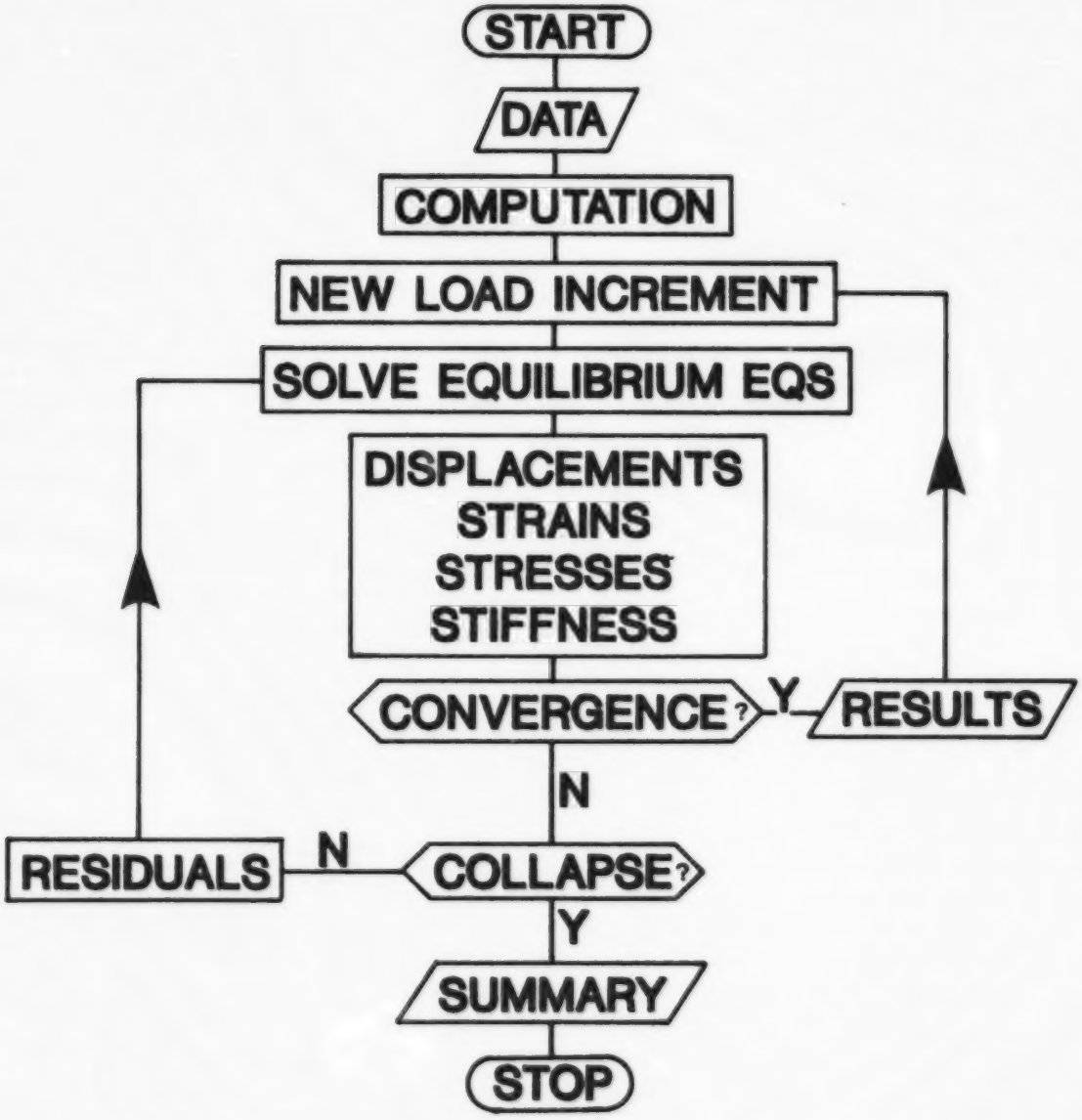

Fig. 14 Flowchart of Program S4

Table 2: Properties of H-Sections Used as Steel Supports

Section	b (mm)	t (mm)	a (mm)	w (mm)	z (mm^3)
H1	76	8.4	76	8.9	42,200
H2	89	9.9	89	9.5	65,600
H3	102	10.3	102	9.5	90,600
H4	114	10.7	114	9.5	121,900
H5	127	13.2	127	10.4	217,087

Yield stress = 268 MPa, E = 200GPa

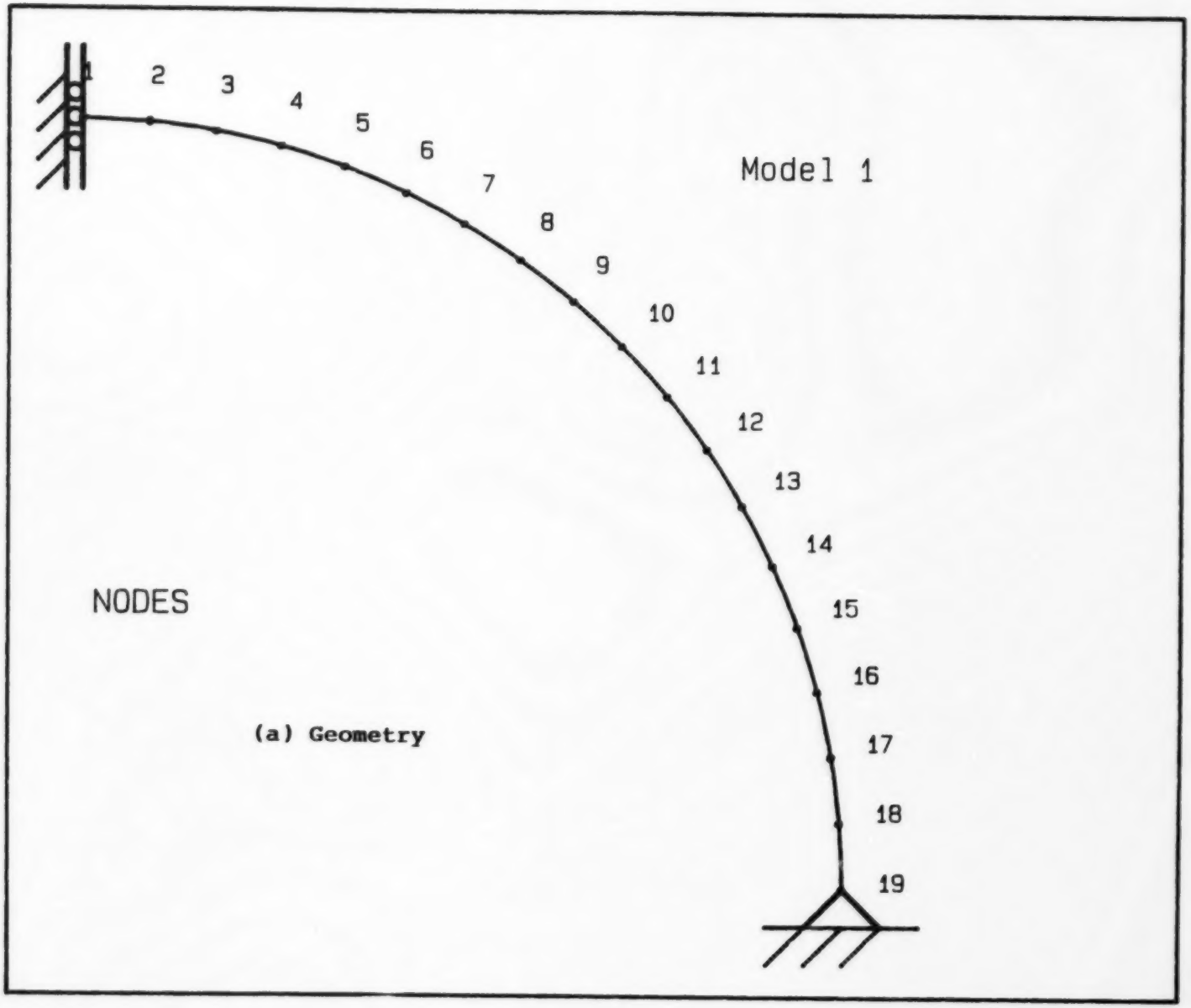
Model 1
1
2
3
4
5
6
7
8
9
10
11
12
13
14
15
16
17
18
19
NODES
(a) Geometry

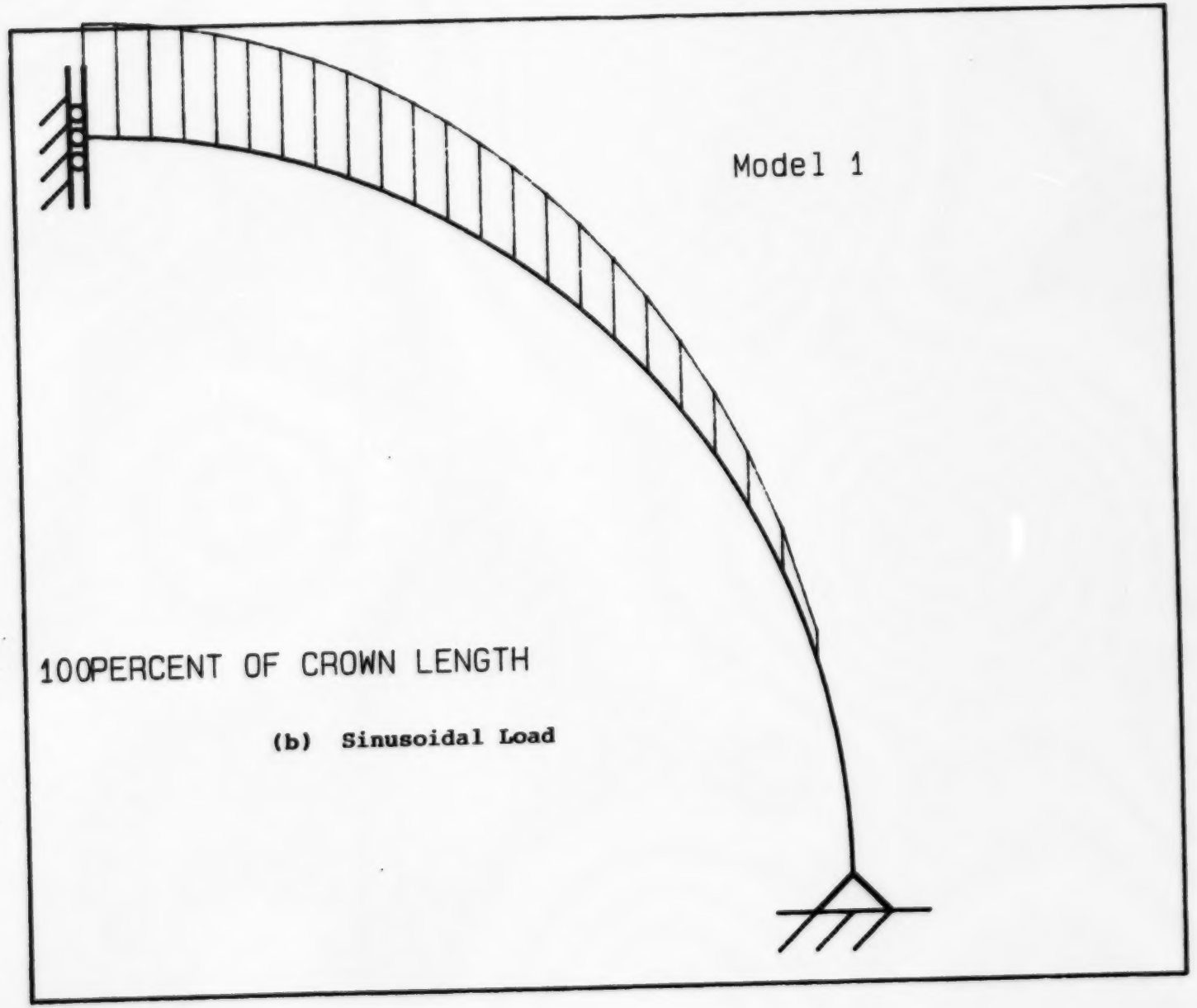

(b) Sinusoidal Load

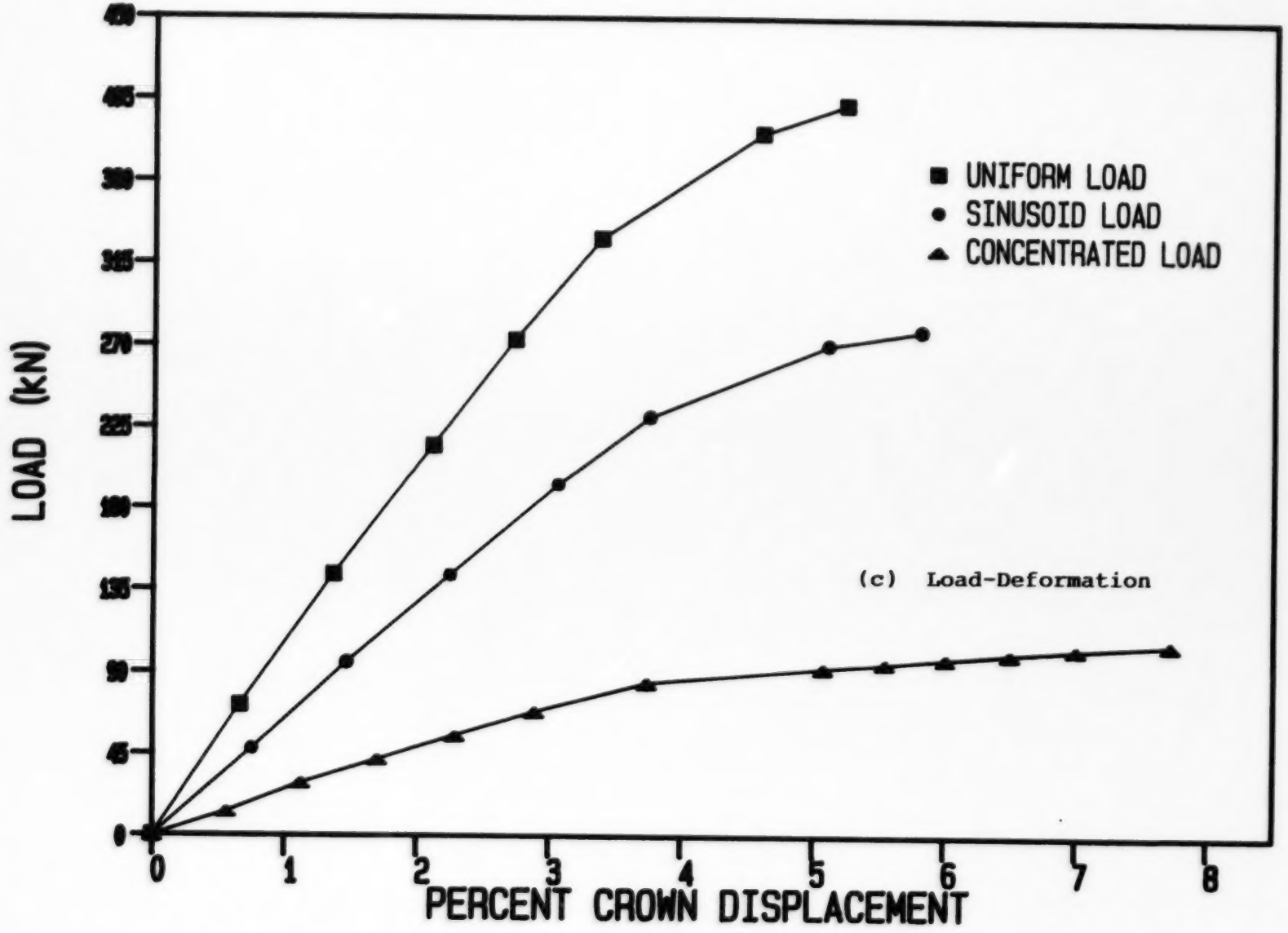

Fig. 15 Data and Results of Model 1

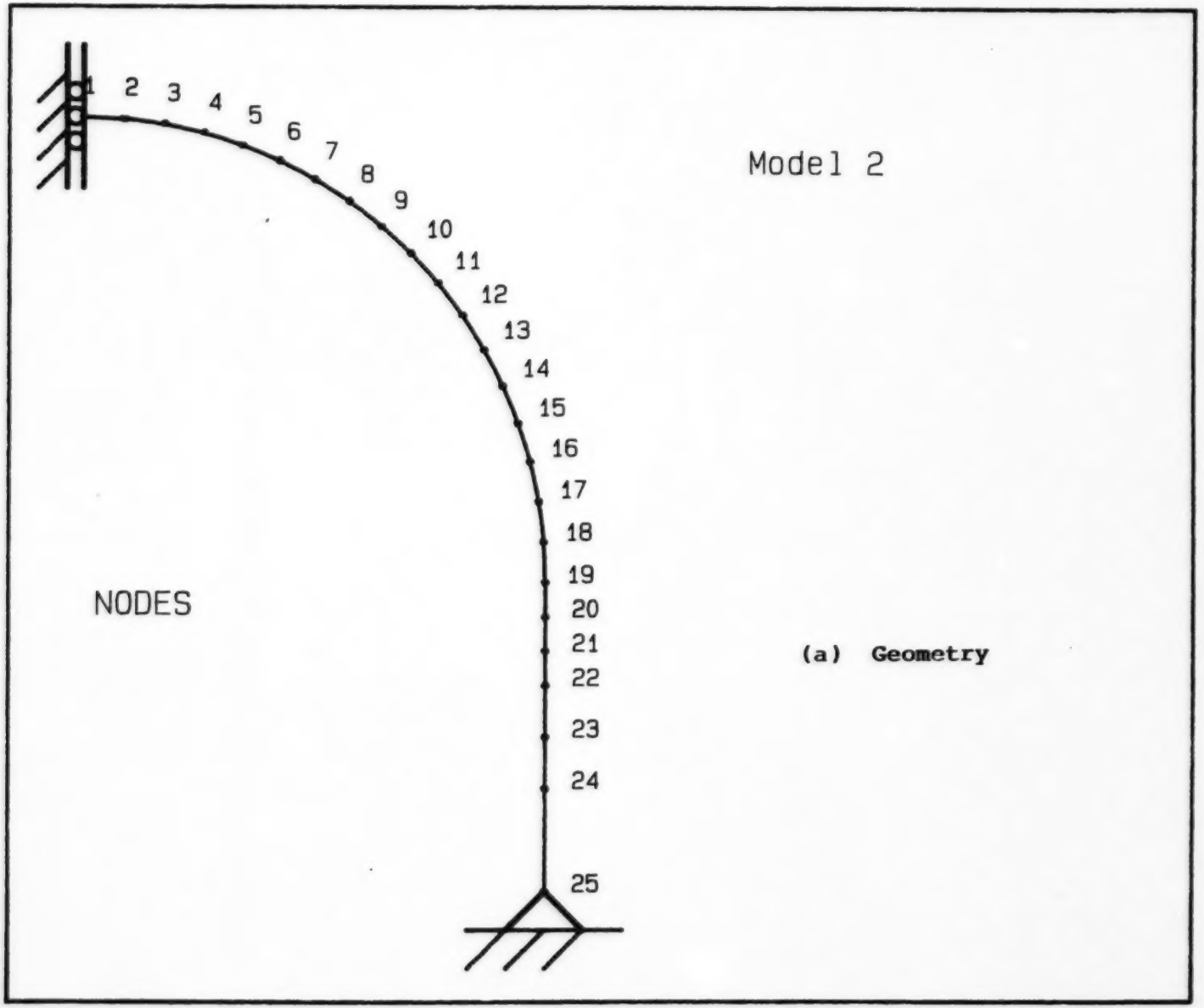
Model 2
NODES
1
2
3
4
5
6
7
8
9
10
11
12
13
14
15
16
17
18
19
20
21
22
23
24
25
(a) Geometry

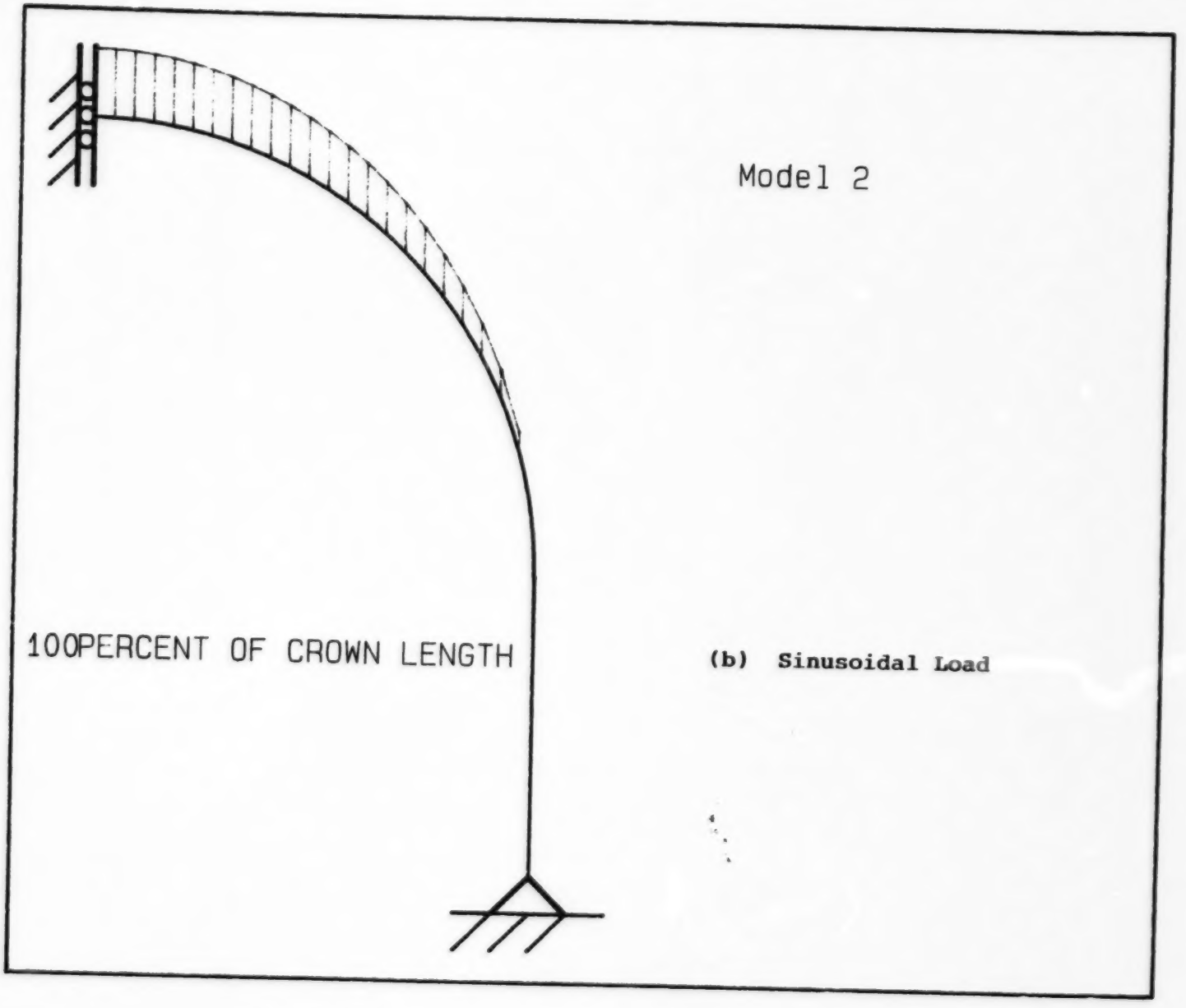
Model 2
100PERCENT OF CROWN LENGTH
(b) Sinusoidal Load

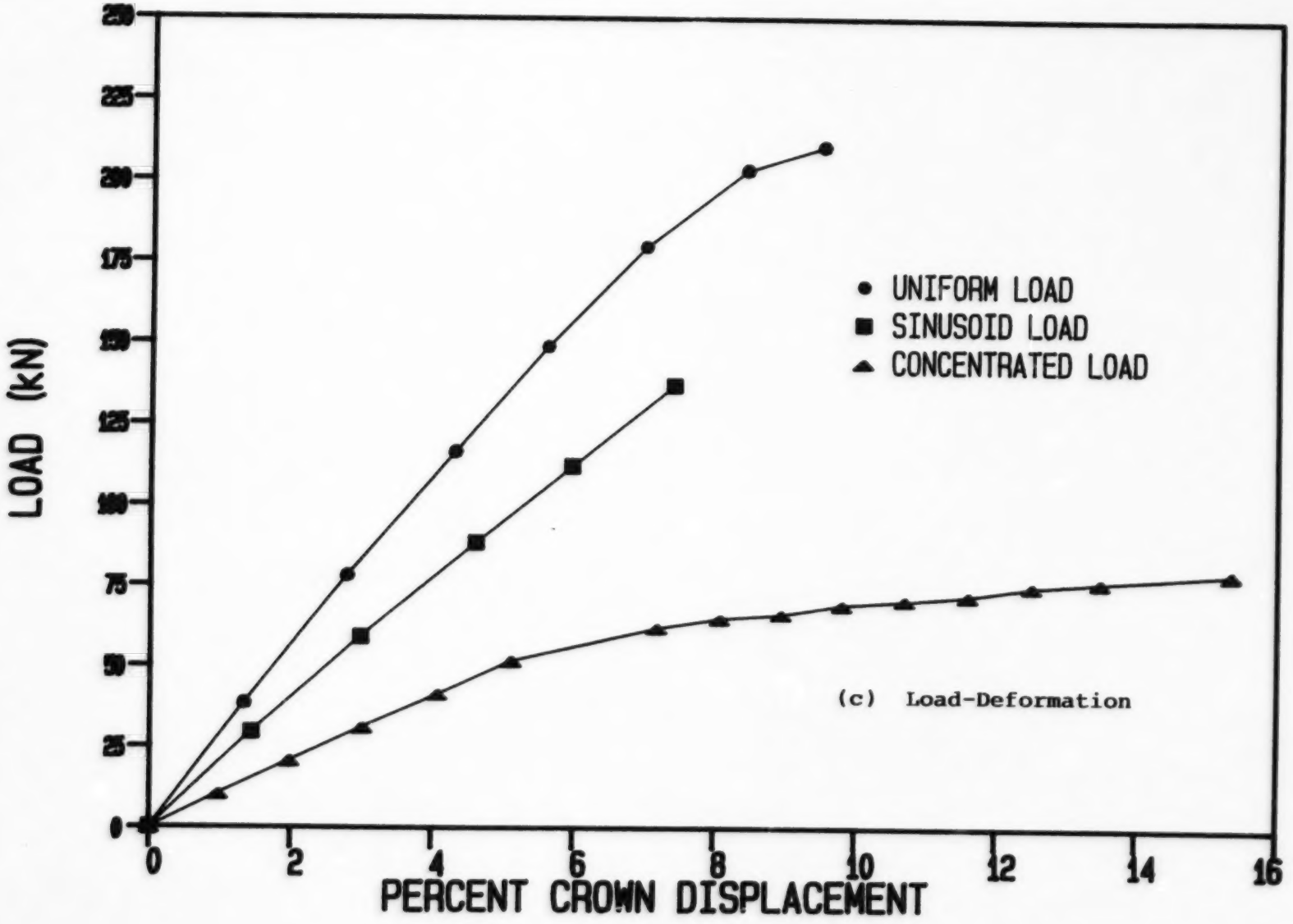

Fig. 16 Data and Results of Model 2

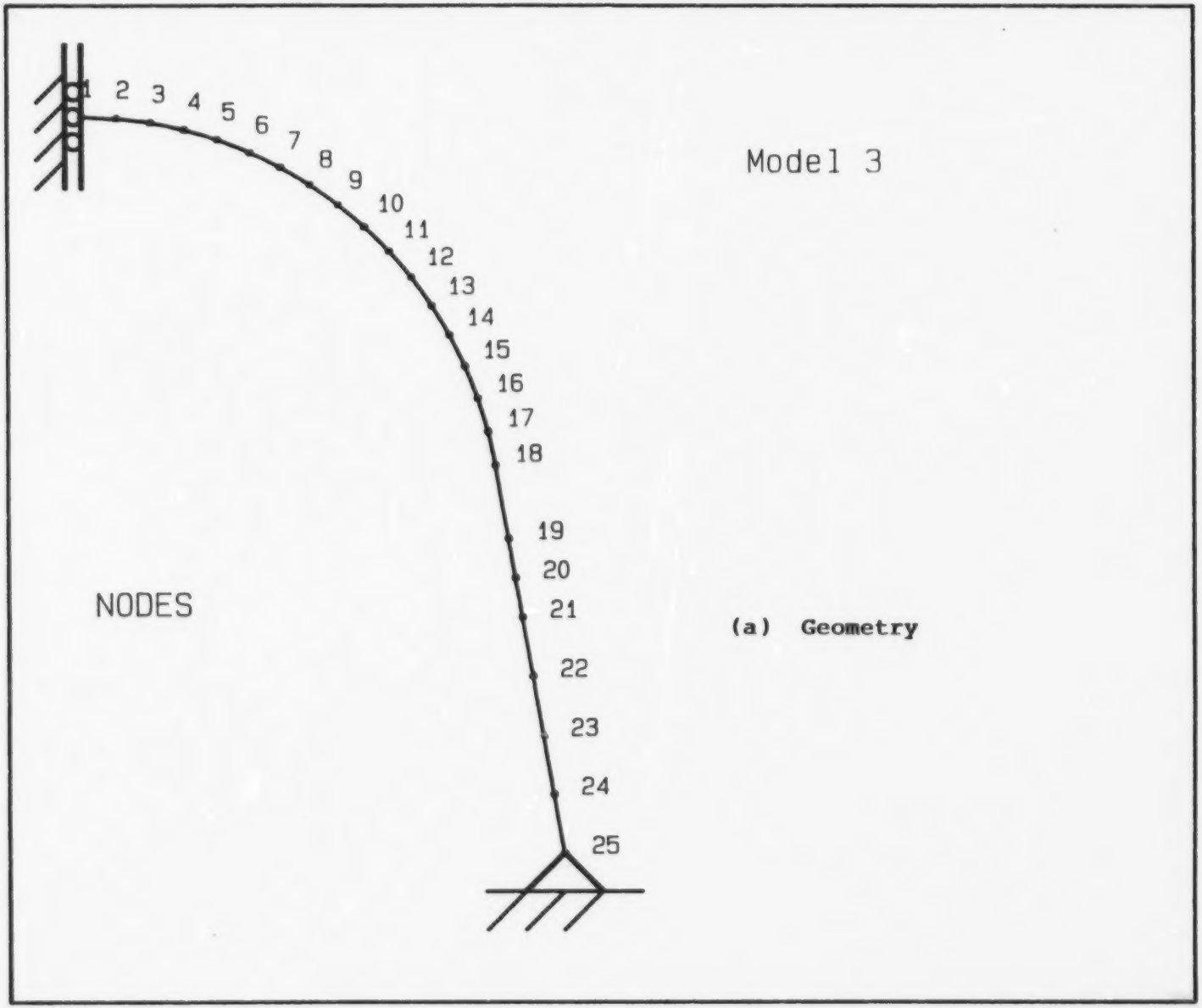
Model 3
NODES
1
2
3
4
5
6
7
8
9
10
11
12
13
14
15
16
17
18
19
20
21
22
23
24
25
(a) Geometry

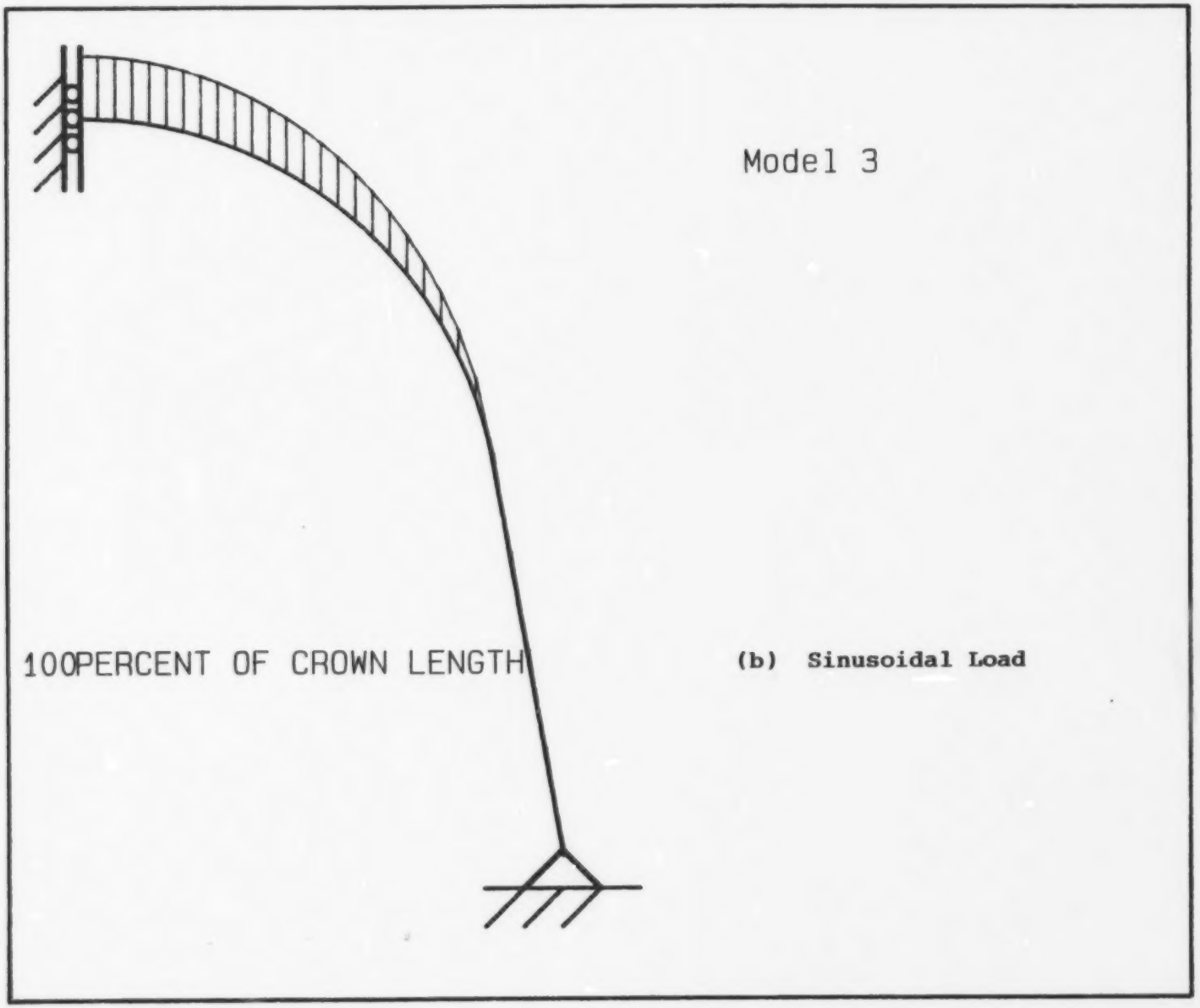

(b) Sinusoidal Load

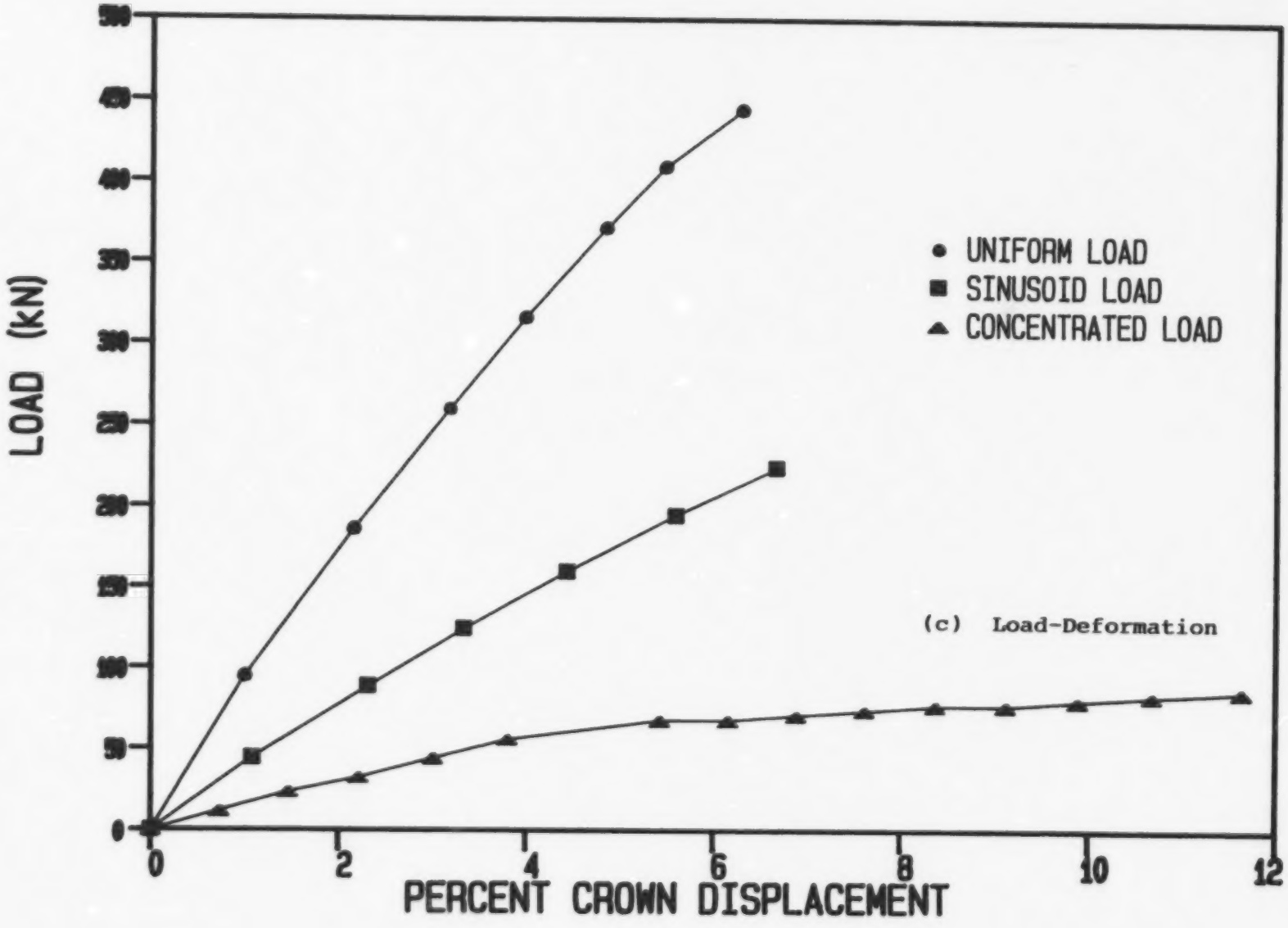

Fig. 17 Data and Results of Model 3

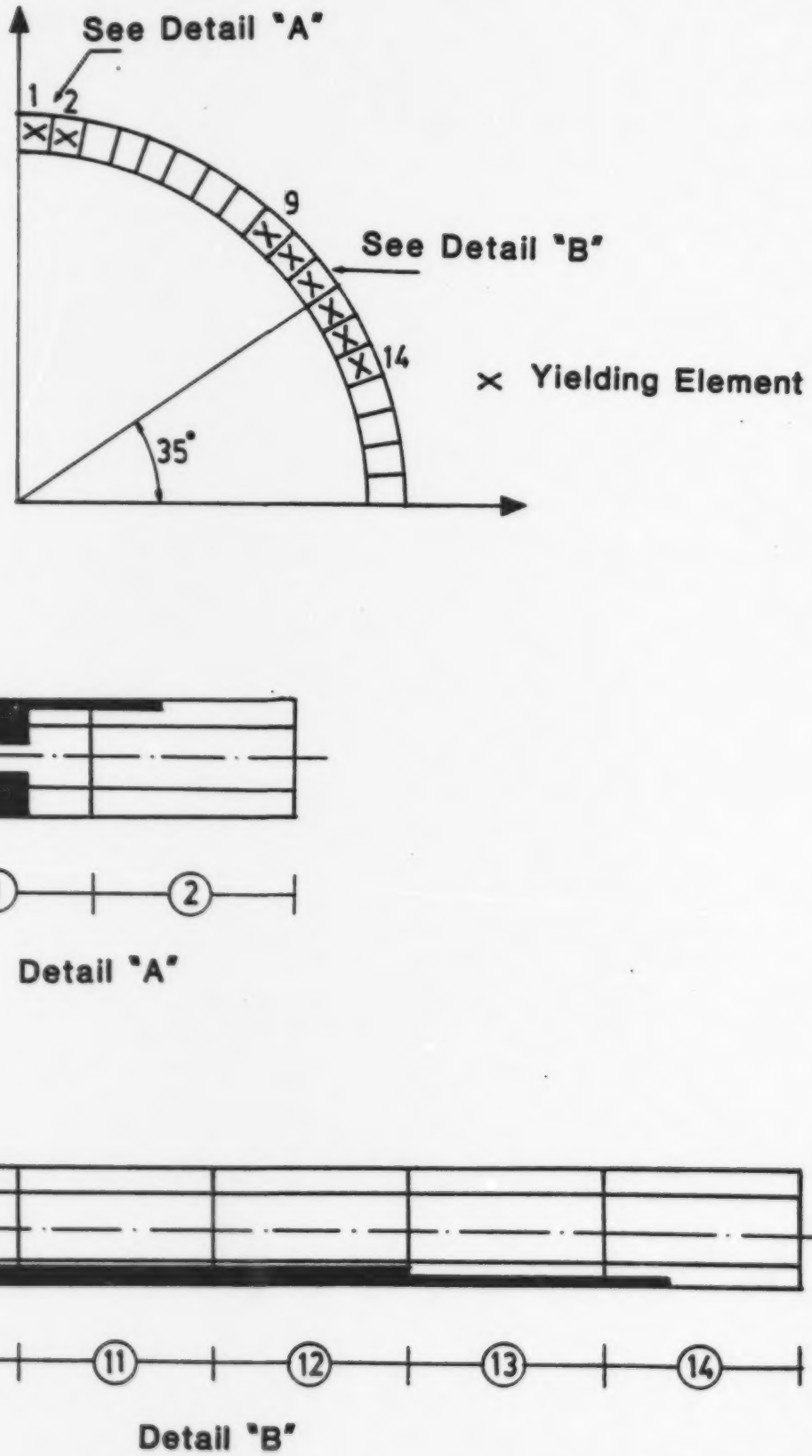

Fig. 18 Distribution of Yield Zones at Failure for a Semicircular Model under Crown Concentrated load

9. CONCLUSIONS

The finite element model that has been developed is capable of simulating the nonlinear behaviour of mine roadway steel arch supports. With the suggested numerical integration scheme, it is possible to trace the progression of plasticity through the element thickness and over its length. An algorithm which is based on measuring the global stiffness deterioration is developed to automate proportional loading of different increment sizes to the point of collapse.

A computer program called S4 has been written and implemented on microcomputer. Examples of support characteristic curves produced by Program S4 have been presented. Full details of the program, the user's information manual and numerical modelling examples will follow in Phase II documentation of this project.

REFERENCES

1. A. Brown, S.G. Campbell, A Comparison of Arches of Different Construction under Single Point Loading. National Coal Board Central Engineering Establishment, Report No. LT 651, (1965).

2. S.L. Paul, C.P. Siess, and E.H. Gaylord, Large Scale Tests of Tunnel Supports. Proceedings of Rapid Excavations and Tunnelling Conference, San Francisco, Vol. 2, (CH. 91), pp. 1395-1417, (1974).

3. H. Cunliffe, A.G. Johnston, Roadway Supports with Special Reference to Yielding Arches. Transactions of the Inst. Mining Engineers, Vol. 117, pp. 804-818, (1957).

4. C. Round, S. Lewis, Royton Drift: New Mine, New Techniques. The Mining Engineer, Vol. 141, pp. 17-24, (1981).

5. S.G. Jukes, F.P. Hassani, and B.N. Whittaker, Characteristics of Steel Arch Support Systems for Mine Roadways, Part I, Modelling Theory, Instrumentation and Preliminary Results. Mining Science and Technology, Vol. 1, pp. 43-58, (1983).

6. F.P. Hassani, A.A. Afrouz, and H.S. Mitri, An Investigation into the Design of Steel Arch Support System in Mine Roadways. 89th Annual General Meeting of CIM, Toronto, Canada (1987).

7. G.A. Morris, and S.J. Fenves, Elastic Plastic Analysis of Frameworks. Struct. Div. ASCE, Vol. 96, No. ST5, pp. 931-946, (1970).

8. B.B. Agyris, U. Hindenlang, and M. Kleiber, Finite Element Analysis of Two and Three-Dimensional Elasto-Plastic Frames - The Natural Approach. Comp. Meth. Appl. Mech. Engng., Vol. 35, pp. 221-248, (1982).

9. M.H. El-Zanaty, and D.W. Murray, Nonlinear Finite Element Analysis of Steel Frames. J. Struct. Div. ASCE, Vol. 109, No. 2, pp. 353-368, (1981).

10. C. Cichon, Large Displacements In-Plane Analysis of Elastic-Plastic Frames. Computers & Structures, Vol.1 9, No. 5/6, pp. 737-745, (1984).

11. Y.C. Fung, A First Course in Continuum Mechanics. 2nd Ed., Prentice Hall Inc., New Jersey, (1977).

12. D.R.J. Owen, and E. Hinton, Finite Element in Plasticity - Theory and Practice. Pineridge Press Ltd., Swansea, U.K., (1980).

13. K-J. Bathe, and A.P. Cimento, Some Practical Procedures for the Solution of Nonlinear Finite Element Equations. Comp. Meth. Appl. Mech. Engng., Vol. 22, pp. 58-85, (1980).

14. K-J. Bathe, and E.N. Dvorkin, On the Automatic Solution of Nonlinear Finite Element Equations. Computers & Sturctures, Vol. 17, No. 5-6, pp. 871-879, (1983).

15. E. Riks, An Incremental Approach to the Solution of Snapping and Buckling Problems. Int. J. Solids Structures, Vol. 15, pp. 529-551, (1979).

16. B. Whittaker and D. Hodgkinson, The incluence of Size on Gate Roadway Stability. The Mining Engineer, January (1971), pp. 203-214.

17. K.-J. Bathe, Finite Element Procedures in Engineering Analysis. Prentice Hall Inc., New Jersey (1982).